ELSEVIER

Brain & Development 34 (2012) 72–75

BRAIN & DEVELOPMENT
Official Journal of the Japanese Society of Child Neurology

www.elsevier.com/locate/braindev

Case report

Paradoxical increase in seizure frequency with valproate in nonketotic hyperglycinemia

Yu Tsuyusaki [a], Hiroko Shimbo [a], Takahito Wada [a], Mizue Iai [a], Megumi Tsuji [a], Sumimasa Yamashita [a], Noriko Aida [b], Shigeo Kure [c], Hitoshi Osaka [a,*]

[a] *Division of Neurology, Kanagawa Children's Medical Center, Yokohama, Japan*
[b] *Division of Radiology, Kanagawa Children's Medical Center, Yokohama, Japan*
[c] *Department of Pediatrics, Graduate School of Medicine, Tohoku University, Sendai, Japan*

Received 31 July 2010; received in revised form 18 December 2010; accepted 10 January 2011

Abstract

Nonketotic hyperglycinemia (NKH), or glycine encephalopathy, is an autosomal recessive disorder caused by a defect in the glycine cleavage enzyme system. In neonatal-onset NKH, patients manifest lethargy, hypotonia, apnea, and intractable epileptic seizures that are not specific to this disease. We experienced a 6-year-old girl with spastic quadriplegia, intractable epilepsy, and mental retardation, all initially regarded as sequelae of neonatal meningitis. The seizure frequency was transiently increased when valproate was started. Head MRI revealed progressive brain atrophy and white matter loss with high intensity signals on T2-weighted and diffusion-weighted images, which prompted us to conduct further metabolic workups. High glycine levels led us to suspect NKH, and we confirmed this diagnosis by the non-invasive, ^{13}C-glycine breath test. DNA sequencing revealed novel Leu885Pro/Trp897Cys mutations in the glycine decarboxylase gene that were transmitted from both parents. Sodium benzoate and dextromethorphan dramatically decreased her hypertonicity. Our case shows that paradoxical increases in seizure frequency following valproate can be a clue for a diagnosis of NKH, and that a correct diagnosis of NKH can greatly alter the quality of life in such patients.

Keywords: Nonketotic hyperglycinemia; Glycine decarboxylase; Glycine encephalopathy; Glycine cleavage system

1. Introduction

Nonketotic hyperglycinemia (NKH), or glycine encephalopathy (MIM #605899), is an autosomal recessive disorder of glycine metabolism caused by a defect in the glycine cleavage enzyme system (GCS), a multienzyme complex located in the inner mitochondrial membrane of the liver, kidney, brain, and placenta. It consists of four individual protein components: P (a pyridoxal phosphate-dependent glycine decarboxylase encoded by the GLDC gene), H (a lipoic acid-containing hydrogen carrier protein encoded by the GCSH gene), T (a tetrahydrofolate-dependent protein encoded by the AMT gene), and L (a lipoamide dehydrogenase encoded by the DLD gene). NKH results from defects only in the P, H, and T components of GCS that lead to high glycine concentrations in urine, plasma, and especially cerebrospinal fluid (CSF) [1,2]. In neonatal-onset NKH, patients manifest lethargy, hypotonia, apnea, and intractable epileptic seizures resulting in profound psychomotor disability [3]. We report the case of a 6-year-old girl with NKH, who was initially diagnosed with cerebral palsy due to neonatal meningitis, and who showed increased seizures following valproic acid (VPA) treatment.

* Corresponding author. Address: Division of Neurology, Clinical Research Institute, Kanagawa Children's Medical Center, Mutsukawa 2-138-4, Minami-ku, Yokohama 232-8555, Japan. Tel.: +81 45 711 2351.
E-mail address: hosaka@kcmc.jp (H. Osaka).

0387-7604/$ - see front matter
doi:10.1016/j.braindev.2011.01.005

2. Patient and methods

2.1. Case history

The patient, now a 6-year-old girl, was born to a healthy mother at 37 weeks of gestation with a birth weight of 3020 g. There is no family history of metabolic disease. The patient was not "doing-well" and showed hypotonia and difficulty in sucking after birth. During the neonatal period, she exhibited frequent seizures resulting in shock and disseminated intravascular coagulation that required mechanical ventilation. As leukocytes counts in the CSF were elevated and serum PCR was positive for type 4 echo-virus-related viruses, she was diagnosed with aseptic meningitis. A brain CT scan at the age of 14 days revealed no abnormalities, including in white matter, or brain destruction. She exhibited repeated generalized seizures and her EEG showed hypsarrhythmia at 1 month. Neither phenobarbital nor Vitamin B6 was effective and she was referred to our hospital for the control of seizures at 5 months. Her head circumference was 42.8 cm (1.57 SD above the mean) and CT revealed enlarged ventricles that were slightly reduced by a ventriculoperitoneal shunt. She was treated with VPA (30 mg/kg, for 2 weeks), after which she experienced fever, rush, and increased frequency of seizures. VPA was discontinued due to what we considered hypersensitivity although the drug lymphocyte stimulation test was negative. Her seizures were not controlled by zonisamide, carbamazepine, or topiramate. When VPA was restarted, the frequency of seizures again increased and the treatment was discontinued. From the age of four, her severe spasticity worsened and diazepam, eperisone, dantrolene, and baclofen were all ineffective; she was re-admitted for the control of hypertonicity and seizures. She could not smile, roll over, or control her head. Her posture was opisthotonic and she could not lie in a supine position. She had severe rigidity and spasticity of the extremities, brisk deep tendon reflexes, a positive Babinski sign, and ankle clonus.

In search of the cause of her apparent regression, we re-evaluated her brain CT/MRI. CT revealed severely dilated ventricles and diffuse brain atrophy with dominantly affected white matter and relatively spared basal nuclei (Fig. 1A). This finding was compatible with post-meningitis hydrocephalus and brain atrophy. Brain MRI revealed progressive brain atrophy and white matter loss with a T2 prolongation of white matter (Fig. 1B). Surprisingly, on the diffusion-weighted image, there was a high intensity signal in the white matter (Fig. 1C).

2.2. Enzymatic analysis

GCS activity was investigated by the ^{13}C-glycine breath test as described previously [4]. Briefly, 10 mg/kg of ^{13}C-glycine was administered through a gastric tube. Breath samples were collected using a face mask equipped with a one-way air valve, and then transferred to a sampling bag. The $^{13}CO_2$ concentrations of the breath samples were measured as described [4].

2.3. RNA, genomic DNA extraction, RT-PCR, and sequencing

Total RNA was extracted from leukocytes using Trizol reagent and subjected to reverse transcription with PrimeScript reverse transcriptase (Invitorogen, Carlsbad, CA) using oligo(dT) primers. RT-PCR was performed using primers that covered the translated region of *GLDC* mRNA (Table 1) and the Ex Taq PCR version 1.0 kit (Takara, Shiga, Japan) according to the manufacturer's instructions (Table 1). Genomic DNA was prepared from white blood cells using the Wizard Genomic DNA purification kit (Promega, Madison, WI). PCR of exons 1, 22, and 23 of the GLDC gene were performed with specific

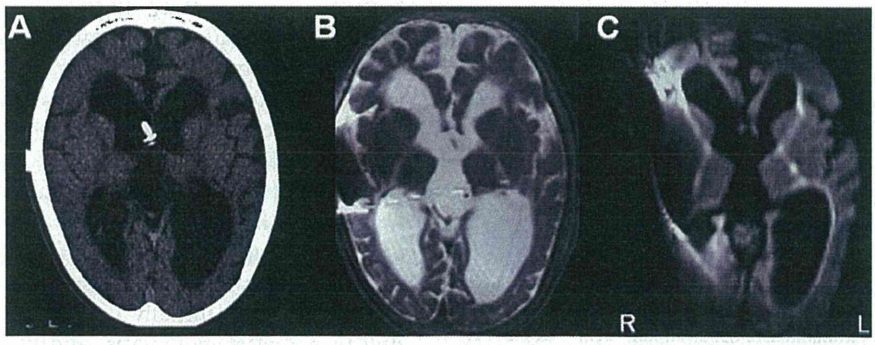

Fig. 1. (A) Brain CT showing severely dilated ventricles and diffuse brain atrophy with dominantly affected white matter and relatively spared basal nuclei, compatible with post-meningitis hydrocephalus and brain atrophy. A ventriculoperitoneal shunt tube was placed in the left lateral ventricle. (B) T2-weighted MRI also showing diffuse brain atrophy with dominantly affected white matter. The T2 prolongation and volume loss of white matter suggested white matter injury. (C) MRI diffusion-weighted image showing a high intensity signal in white matter, suggesting white matter degeneration. Please note that the ventriculoperitoneal shunt valve causes the defects and flaring of images.

Table 1
Primers and conditions for PCR.

Name	Primer	Position	Sequence	Size of PCR product (bp)	Annealing temperature (°C)
GLDC 1F	Sense	Exon1	5′-AAAGACCAGAGAGAGATGCT-3′	719	65⇒60*
GLDC 1R	Antisense	Exon7	5′-ATGTCTACCCCAAATTCTCCA-3′		
GLDC 2F	Sense	Exon6	5′-GAAAAGATGTCAGTGGAGTGT-3′	720	65⇒60*
GLDC 2R	Antisense	Exon11/12	5′-GTTCTGCAGATGACTCACAAC-3′		
GLDC 3F	Sense	Exon10	5′-GCATCAACTCCAGCATGACC-3′	682	60
GLDC 3R	Antisense	Exon17	5′-GGTCCCATGTGCTGATTTCG-3′		
GLDC 4F	Sense	Exon15	5′-AGGATATCAGCAGCTTTTCC-3′	718	60
GLDC 4R	Antisense	Exon21	5′-TTGTTTAAGACCCTTGCCTC-3′		
GLDC 5F	Sense	Exon19/20	5′-TCGGAGTGAAGAAACATCTC-3′	743	60
GLDC 5R	Antisense	Exon25	5′-CCTCTTTTGTTCAGAAAATGGAG-3′		
GLDC 6F	Sense	Exon23	5′-TGATCAGCATTCGGCAGGAAA-3′	622	60
GLDC 6R	Antisense	Exon25	5′-TCTCCAGGATAGCCTCTATGACA T-3′		
GLDCex22F	Sense	Intron21	5′-ACATAAAAAGCTGATGCACT-3′	345	60
GLDCex22R	Antisense	Intron22	5′-CTATTATTTTGGAGGTTGCC-3′		
GLDCex23F	Sense	Intron22	5′-TTCTATGAACAGCACTGAGA-3′	434	60
GLDCex23R	Antisense	Intron23	5′-GTATCATCCTCAGTTGAGAG-3′		

primers using Ex Taq PCR version 1.0 kit (Takara, Shiga, Japan) according to the manufacturer's instructions (Table 1). The PCR fragments were sequenced using the Big Dye Terminators v1.1 Cycle Sequencing kit (Applied Biosystems, Foster City, CA).

3. Results

From the MRI findings, we suspected a metabolic disorder causing white matter degeneration. Leukocyte lysosomal enzyme activities, including arylsulfatase A, were normal. Bone marrow revealed normocellularity without foam cells. Amino acid analysis of plasma revealed a substantially high level of glycine (1671.1 nmol/ml, normal range: 127–341) with high CSF/plasma glycine levels (266.8/2074.5 nmol/ml, normal range: 4.8–8.4/127–341). The elevated glycine and characteristic white matter tract abnormalities revealed by diffusion-weighted (DWI) in patients with NKH [5], led us to conduct the ^{13}C-glycine breath test. This showed a significantly decreased ^{13}C-cumulative recovery of only 13.1% (<−2SD), strongly suggesting NKH [4]. RT-PCR and subsequent sequencing revealed Leu885Pro/Trp897Cys missense mutations in *GLDC* that were transmitted from both parents

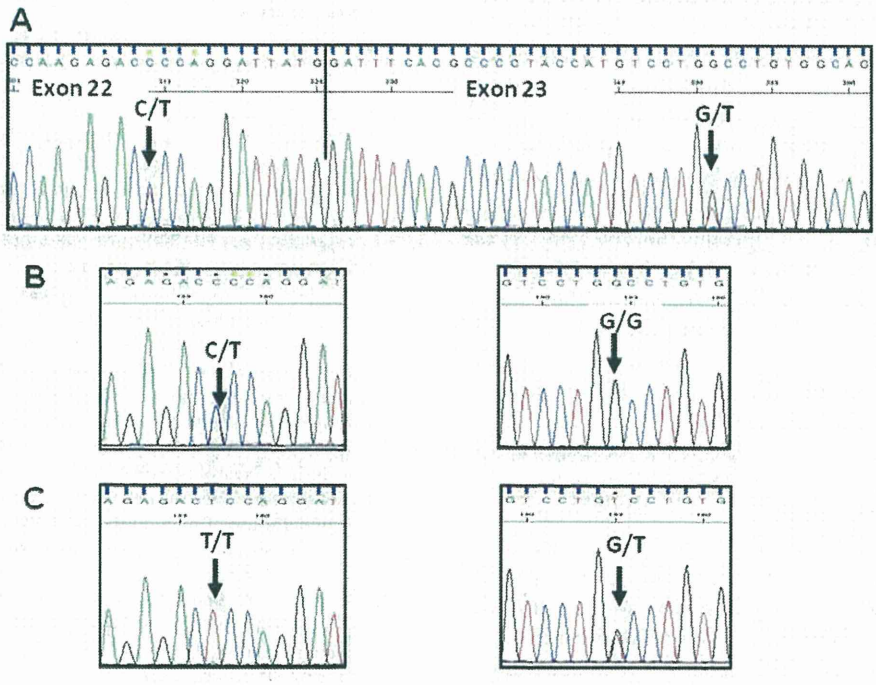

Fig. 2. (A) RT-PCR and subsequent sequencing showed heterozygous Leu885Pro/Trp897Cys missense mutations of the GLDC gene. Sequencing genomic DNA from her parents revealed that these mutations were transmitted from her mother (B), and father (C).

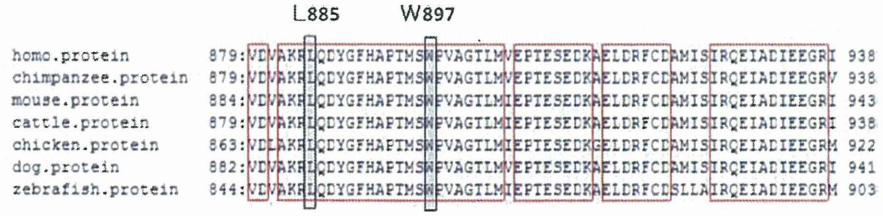

Fig. 3. Patient's GLDC amino acid sequence compared with that of several other animals reveals that both substituted residues Leu885 and Trp897 are highly conserved among species.

(Fig. 2). These mutations should not be polymorphisms, because both residues are highly conserved among species (Fig. 3) and we did not detect them in more than 100 control alleles. After we diagnosed the patient with NKH, we started sodium benzoate (250 mg/kg) and dextromethorphan (20 mg/kg). She showed dramatically decreased hypertonicity and now goes to a special elementary school.

4. Discussion

NKH is often erroneously diagnosed as sepsis or hypoxic ischemic injury, particularly in the severe neonatal cases [3,6]. In the present case, septic meningitis with echo-related virus made the correct diagnosis of NKH difficult. Seizure frequencies were increased following both occasions of VPA therapy. VPA reduces GCS activity and inhibits glycine uptake to mitochondria and increases the level of glycine in serum and CSF in NKH patients [7,8]. Excessive stimulation by glycine of the excitatory N-methyl-D-aspartate (NMDA)-type glutamate receptor causes the seizures and possible excitotoxicity characteristic of NKH [9]. That raised the possibilities that the VPA therapy elevated the level of glycine and exaggerated the neurological presentation in this patient. A somewhat similar case report describes a patient with nonketotic hyperglycinemia following her presentation with acute encephalopathy and chorea shortly after initiation of valproate therapy [10]. As far as we know, increases in seizure frequencies after administration of VPA have not been reported in the English literature. This patient again teaches us to consider a differential diagnosis of NKH in patients showing paradoxical worsening of neurological status such as seizure frequency following VPA.

Benzoate decreases glycine levels by conjugation and excretion as hippurate glycine. Dextromethorphan, converted to its active metabolite, dextrorphan, acts as a noncompetitive inhibitor of the NMDA receptor [9]. Sodium benzoate and dextromethorphan dramatically decreased the patient's hypertonicity and seizure frequency. Although NKH is an incurable disease, a correct diagnosis altered the patient's life completely, enabling her to leave hospital, return home, and to attend school, thus emphasizing the importance of a correct diagnosis of NKH.

Acknowledgements

This work was supported in part by Grants-in-Aid for Scientific Research from the Ministry of Health, Labor and Welfare of Japan, Health and Labor Science Research Grant of Japan, Takeda Science Foundation, and Kanagawa Municipal Hospital Pediatric Research.

References

[1] Kikuchi G, Motokawa Y, Yoshida T, Hiraga K. Glycine cleavage system: reaction mechanism, physiological significance, and hyperglycinemia. Proc Jpn Acad Ser B Phys Biol Sci 2008;84:246–63.
[2] Kure S, Kato K, Dinopoulos A, Gail C, DeGrauw TJ, Christodoulou J, et al. Comprehensive mutation analysis of GLDC, AMT, and GCSH in nonketotic hyperglycinemia. Hum Mutat 2006;27:343–52.
[3] Korman SH, Gutman A. Pitfalls in the diagnosis of glycine encephalopathy (non-ketotic hyperglycinemia). Dev Med Child Neurol 2002;44:712–20.
[4] Kure S, Korman SH, Kanno J, Narisawa A, Kubota M, Takayanagi T, et al. Rapid diagnosis of glycine encephalopathy by ^{13}C-glycine breath test. Ann Neurol 2006;59:862–7.
[5] Mourmans J, Majoie CB, Barth PG, Duran M, Akkerman EM, Poll-The BT. Sequential MR imaging changes in nonketotic hyperglycinemia. AJNR Am J Neuroradiol 2006;27:208–11.
[6] Hoover-Fong JE, Shah S, Van Hove JL, Applegarth D, Toone J, Hamosh A. Natural history of nonketotic hyperglycinemia in 65 patients. Neurology 2004;63:1847–53.
[7] Kochi H, Hayasaka K, Hiraga K, Kikuchi G. Reduction of the level of the glycine cleavage system in the rat liver resulting from administration of dipropylacetic acid: an experimental approach to hyperglycinemia. Arch Biochem Biophys 1979;198:589–97.
[8] Simila S, von Wendt L, Linna SL. Dipropylacetate and aminoaciduria. J Neurol Sci 1980;45:83–6.
[9] Hamosh A, Maher JF, Bellus GA, Rasmussen SA, Johnston MV. Long-term use of high-dose benzoate and dextromethorphan for the treatment of nonketotic hyperglycinemia. J Pediatr 1998;132:709–13.
[10] Morrison PF, Sankar R, Shields WD. Valproate-induced chorea and encephalopathy in atypical nonketotic hyperglycinemia. Pediatr Neurol 2006;35:356–8.

Molecular Genetics and Metabolism 105 (2012) 553–558

Contents lists available at SciVerse ScienceDirect

Molecular Genetics and Metabolism

journal homepage: www.elsevier.com/locate/ymgme

Simple and rapid genetic testing for citrin deficiency by screening 11 prevalent mutations in *SLC25A13*

Atsuo Kikuchi [a,*], Natsuko Arai-Ichinoi [a], Osamu Sakamoto [a], Yoichi Matsubara [b], Takeyori Saheki [c,1], Keiko Kobayashi [d], Toshihro Ohura [e], Shigeo Kure [a]

[a] Department of Pediatrics, Tohoku University Graduate School of Medicine, 1-1 Seiryo-machi, Aoba-ku, Sendai, Miyagi 980-8574, Japan
[b] Department of Medical Genetics, Tohoku University School of Medicine, 1-1 Seiryo-machi, Aoba-ku, Sendai, Miyagi 980-8574, Japan
[c] Institute for Health Sciences, Tokushima Bunri University, 180 Yamashiro-cho, Tokushima 770-8514, Japan
[d] Department of Molecular Metabolism and Biochemical Genetics, Kagoshima University, Kagoshima 890-8544, Japan
[e] Division of Pediatrics, Sendai City Hospital, 3-1 Shimizukoji, Wakabayashi-ku, Sendai, Miyagi 984-8501, Japan

ARTICLE INFO

Article history:
Received 13 November 2011
Received in revised form 29 December 2011
Accepted 30 December 2011
Available online 8 January 2012

Keywords:
Citrin deficiency
Genetic diagnosis
Rapid diagnosis
Expanded newborn screening
SLC25A13

ABSTRACT

Citrin deficiency is an autosomal recessive disorder caused by mutations in the *SLC25A13* gene and has two disease outcomes: adult-onset type II citrullinemia and neonatal intrahepatic cholestasis caused by citrin deficiency. The clinical appearance of these diseases is variable, ranging from almost no symptoms to coma, brain edema, and severe liver failure. Genetic testing for *SLC25A13* mutations is essential for the diagnosis of citrin deficiency because chemical diagnoses are prohibitively difficult. Eleven *SLC25A13* mutations account for 95% of the mutant alleles in Japanese patients with citrin deficiency. Therefore, a simple test for these mutations is desirable. We established a 1-hour, closed-tube assay for the 11 *SLC25A13* mutations using real-time PCR. Each mutation site was amplified by PCR followed by a melting-curve analysis with adjacent hybridization probes (HybProbe, Roche). The 11 prevalent mutations were detected in seven PCR reactions. Six reactions were used to detect a single mutation each, and one reaction was used to detect five mutations that are clustered in a 21-bp region in exon 17. To test the reliability, we used this method to genotype blind DNA samples from 50 patients with citrin deficiency. Our results were in complete agreement those obtained using previously established methods. Furthermore, the mutations could be detected without difficulty using dried blood samples collected on filter paper. Therefore, this assay could be used for newborn screening and for facilitating the genetic diagnosis of citrin deficiency, especially in East Asian populations.

1. Introduction

Citrin deficiency is an autosomal recessive disorder that results from mutations in the *SLC25A13* gene [1] and causes two diseases: adult-onset type II citrullinemia (CTLN2; OMIM #603471) and neonatal intrahepatic cholestasis caused by citrin deficiency (NICCD; OMIM#605814) [1–4]. The clinical appearance of these diseases is variable and ranges from almost no symptoms to coma, brain edema, and severe liver failure requiring transplantation [5–8]. In a study of patients with NICCD, only 40% of individuals were identified by newborn screenings to have abnormalities, such as hypergalactosemia, hypermethioninemia, and hyperphenylalaninemia [9]. Other patients were referred to hospitals with suspected neonatal hepatitis or biliary atresia, due to jaundice or discolored stool [9]. Hypercitrullinemia was not observed in all patients [9]. Mutation analysis of *SLC25A13* is indispensable because of the difficulties associated with the chemical diagnosis of citrin deficiency. The *SLC25A13* mutation spectrum in citrin deficiency is heterogeneous, and more than 31 mutations of *SLC25A13* have been identified to date [1,10–18]. However, there are several predominant mutations in patients from East Asia. As shown in Table 1, 6 prevalent mutations account for 91% of the mutant alleles in the Japanese population [12,19]. Five additional mutations also occur within a 21-bp cluster in exon 17 (Table 1 and Fig. 1D). The six prevalent mutations, together with the five mutations in exon 17, account for 95% of the mutant alleles in Japan [12,19].

Several different methods, such as direct sequencing, PCR restriction fragment length polymorphism (PCR-RFLP), and denaturing high performance liquid chromatography (DHPLC), are currently used for the detection of mutations in *SLC25A13* [1,10–14,19]. However, these methods are too complex for clinical use. Direct sequencing is a standard but cumbersome method. The PCR-RFLP method is

Abbreviations: CTLN2, adult-onset type II citrullinemia; FRET, fluorescence resonance energy transfer; HRM, high resolution melting; NICCD, neonatal intrahepatic cholestasis caused by citrin deficiency; Tm, melting temperature.

* Corresponding author. Fax: +81 22 717 7290.
E-mail address: akikuchi-thk@umin.ac.jp (A. Kikuchi).
[1] Present address: Institute of Resource Development and Analysis, Kumamoto University, Kumamoto 860-0811, Japan.

1096-7192/$ – see front matter © 2012 Elsevier Inc. All rights reserved.
doi:10.1016/j.ymgme.2011.12.024

Table 1
Seven primer/probe sets and 11 targeted mutations of *SLC25A13*.

Primer/probe set	Mutation		Location	Nucleotide change	Effects of mutations	Allele frequency* [19]	References
A	Mutation [I]	:851del4	exon 9	c.851_854delGTAT	p.R284fs(286X)	33.2%	[1]
B	Mutation [II]	:g.IVS11+1G>A	intron 11	c.1019_1177del	p.340_392del	37.6%	[1]
C	Mutation [III]	:1638ins23	exon 16	c.1638_1660dup	p.A554fs(570X)	3.4%	[1]
D	Mutation [IV]	:S225X	exon 7	c.675C>A	p.S225X	5.3%	[1]
E	Mutation [V]	:g.IVS13+1G>A	intron 13	c.1231_1311del	p.411_437del	8.2%	[1]
F	Mutation [XIX]	:IVS16ins3kb	intron 16	c. aberrant RNA	p.A584fs(585X)	4.6%	[19]
G	Mutation [VI]	:1800ins1	exon 17	c.1799_1800insA	p.Y600X	1.3%	[10]
	Mutation [VII]	:R605X	exon 17	c.1813C>T	p.R605X	0.90%	[10]
	Mutation [VIII]	:E601X	exon 17	c.1801G>T	p.E601X	1.2%	[11]
	Mutation [IX]	:E601K	exon 17	c.1801G>A	p.E601K	0.30%	[11]
	Mutation [XXI]	:L598R	exon 17	c.1793T>G	p.L598R	0%	[15]
						Total 95.1%	

* The frequency of each mutant allele among Japanese patients with citrin deficiency.

complicated and can lead to genotyping errors, due to incomplete digestion by the restriction enzymes. DHPLC is time-consuming and requires expensive equipment. Thus, there is a strong need for the development of a simple test for these mutations.

The goal of this study was to establish a rapid and simple test for the detection of the 11 most common *SLC25A13* mutations. We adopted the HybProbe format (Roche) for the detection of the mutations using real-time PCR followed by a melting-curve analysis with adjacent hybridization probes [20,21]. This assay can be completed in less than 1 h and has the advantage of being a closed-tube assay. The fundamental process for detecting point mutations using the HybProbe assay is presented in Fig. 1A. The 11 prevalent mutations contain not only point mutations but also include a 4-bp deletion and insertions of 1-bp, 23-bp and 3-kb genomic fragments (Table 1 and Fig. 1). Careful design of the PCR primers and HybProbes enabled us to test for these various *SLC25A13* mutations.

2. Methods

2.1. Subjects

CTLN2 and NICCD were diagnosed, as previously described [9,10,19,22–24]. Genomic DNA of the patients was obtained from peripheral blood leukocytes using the DNeasy blood kit (Qiagen Inc., Valencia, CA, USA). Genomic DNA was purified from filter paper blood samples using the ReadyAmp Genomic DNA Purification System (Promega, Madison, WI, USA). Mutations in these DNA samples were analyzed at Kagoshima University using a combination of PCR with or without restriction enzyme digestion or by direct sequencing, as previously described [1,10–14,19]. Another set of samples was obtained from 420 healthy volunteers (mainly from Miyagi prefecture in the northeastern region of Japan) at Tohoku University. Genomic DNA from leukocytes was extracted, as described above.

2.2. Detection of seven prevalent mutations in SLC25A13 using the HybProbe assay

HybProbe probes comprise a pair of donor and acceptor oligonucleotide probes designed to hybridize adjacent to their target sites in an amplified DNA fragment [20,21]. The donor probes are labeled at their 3′ end with fluorescein isothiocyanate (FITC), whereas the acceptor probes are labeled at their 5′ end with LC Red640; these acceptor probes are phosphorylated at their 3′ end to prevent extension by the DNA polymerase. When two probes hybridize to the amplicon, the fluorescent dyes are located within 5 bases of each other, which allows fluorescence resonance energy transfer (FRET) between the excited FITC and the LC Red640; this process emits light that can be quantified by real-time PCR. Following PCR amplification, a melting-peak analysis is performed. The melting peak is produced by the reporter probe, which has a lower melting temperature (Tm) than the other probe, called the anchor probe. As the reporter melts from the target, the fluorophores are separated, and the FRET ceases. The Tm of the reporter probe determines the reaction

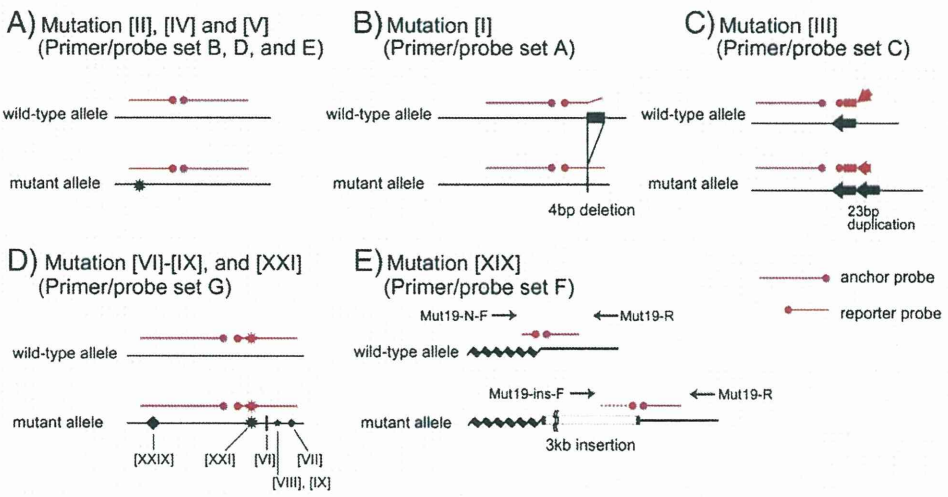

Fig. 1. Principle of *SLC25A13* mutation detection by melting-curve analysis with the HybProbe assay. In primer/probe sets A–E, and G, PCR was performed with a pair of primers, whereas in primer/probe set F, two forward primers and one common reverse primer were used for the amplification of both wild-type and mutant alleles. Note that mutation [XXIX], located on the anchor probe of primer/probe set G, is a non-target mutation.

specificity (i.e., binding of the probe to a perfectly matched sequence rather than to regions with sequence mismatches).

Seven primer/probe sets were designed for this study. Fig. 1 shows a schematic diagram of the strategy for mutation detection using these primer/probe sets. Tables 1 and 2 list the primer/probe sets and corresponding sequences and primer concentrations that were used to target the 11 mutations. Primer/probe sets A, B, C, D, E, and F were designed to detect mutations [I], [II], [III], [IV], [V], and [XIX], respectively. Primer/probe set G was designed to detect the five mutations clustered on exon 17: mutations [VI], [VII], [VIII], [IX], and [XXI] (Fig. 1D). All primers and probes were synthesized based on the NCBI reference SLC25A13 gene sequence (GenBank accession no. **NM_014251**) with the exception of mutation [XIX]:IVS16ins3kb, which was designed according to [19].

Real-time PCR and subsequent melting curve analyses were performed in a closed tube using a 20-μL mixture on a LightCycler 1.5 (Roche Diagnostics, Tokyo, Japan). The PCR mixture contained 2.0 μL of genomic DNA (10–50 ng), 0.5 μM of forward primer, 0.5 or 0.1 μM of reverse primer, 0.2 μM of each sensor and anchor probe, and 10 μL of Premix ExTaq™ (Perfect Real Time) reagent (TaKaRa Bio Inc., Otsu, Japan).

The thermal profile conditions were identical for all seven assays and consisted of an initial denaturation step (30 s at 95 °C), followed by 45 amplification cycles with the following conditions: denaturation for 5 s at 95 °C and annealing and extension for 20 s at 60 °C. The transition rate between all steps was 20 °C/s. After amplification, the samples were held at 37 °C for 1 min, followed by the melting curve acquisition at a ramp rate of 0.15 °C/s extending to 80 °C with continuous fluorescence acquisition.

Table 2
Primers, probes and target amplicon sequences, target mutation sites, and primer concentrations.

Primer/probe set	Name	Sequences of PCR products, primer locations, probe sequences, and mutation sites (5′ to 3′)	Concentration (μmol/L)
A		GGCTATACTGAAATATGAGAAatgaaaaaagggatgtttttaaattttataatgtaaattgtaataaattggtatatttgttgcttgtgtttgtttttcccctacagac	
		gtatgaccttagcagacattgaacggattgctcctctggaagagggaactctgccCTTTAACTTGGCTGAGG (181 bp)	
	Mut1-F	GGCTATACTGAAATATGAGAA	0.5
	Mut1-R	CCTCAGCCAAGTTAAAG	0.5
	Mut1-UP	ATGTAAATTGTAATAAATTGGTATATTTGTTGCTTGTGTT-FITC	
	Mut1-DW	LC Red640-GTTTTTCCCCTACAGAC**GACC**-P	
B		GAATGCAGAACCAACGAtcaactggctcttttgtgggagaactcatgtataaaaacagctttgactgttttaagaaagtgctacgctatgaaggcttctt	
		tggactgtatagaggttagtgccacatgctcaatacctgttaggtgaaataacactcaaaggtttggtttctcatcttagtgcctGACATGAATTAGCAAGACTG (205 bp)	
	Mut2-F	GAATGCAGAACCAACGA	0.5
	Mut2-R	CAGTCTTGCTAATTCATGTC	0.1
	Mut2-UP	ACCTAACAGGTATTGAGCATGTG-FITC	
	MUt2-DW	LC Red640-CACTAA**C**CTCTATACAGTCCA-P	
C		GCAGTTCAAAGCACAGTTATTtttatatagtgagaatgtgaccagactgagatggtgttgtgtctctcctgcaggtatgcctgcagcatctttagtg	
		accccctgctgatgttatcaagacgagattacaggtg	
		gctgcccggg(**gagatta**caggtggctgcccggg)ctggccaaaccaCTTACAGCGGAGTGATAGAC (175 bp)	
	Mut3-F	GCAGTTCAAAGCACAGTTATT	0.5
	Mut3-R	GTCTATCACTCCGCTGTAAG	0.5
	Mut3-UP	ACCCCTGCTGATGTTATCAAGACGAGATTACAGGT-FITC	
	Mut3-DW	LC Red640-GCTGCCCGGG**GAGATTA**-P	
D		TCAATTTATTTGAGGCTGCtggaggtaccacatcccatcaagttagtttctcctattttaatggatttaattcgctccttaacaac	
		atggaactcattagaaagatctatagcactc	
		tggctggcaccaggaaagatgttgaagtGACTAAGGGTGAGTGAGAA (164 bp)	
	Mut4-F	TCAATTTATTTGAGGCTGC	0.5
	Mut4-R	TTCTCACTCACCCTTAGTC	0.5
	Mut4-UP	AATGGATTTAATT**C**GCTCCTTAACA-FITC	
	Mut4-DW	LC Red640-ATGGAACTCATTAGAAAGATCTATAGCACTC-P	
E		TGCACAAAGATGGTTCGgtcccacttgcagcagaaattcttgctggaggctgcgtaagtacctttgaagctctcttcattgaaaagacttgtttcac	
		atatatatcactaccatggtcaacaggtgtggactaaggcttctgttTAACCACAGATCCTGCA (162 bp)	
	Mut5-F	TGCACAAAGATGGTTCG	0.5
	Mut5-R	TGCAGGATCTGTGGTTA	0.5
	Mut5-UP	GTGAAACAAGTCTTTTCAATGAAGAGAGCTTC-FITC	
	Mut5-DW	LC Red640-AAGGTACTTAC**G**CAGCCTC-P	
F	normal allele	GGAGCTGGTGGTATGGAAataatgtgttcttaactaactctttggtatcaggtaaatttttaaaatatctaattatatctgtgatttctc	
		catttttttaaagctcgtgtatttcgatcctcaccccagtttggt	
		gtaactttgctgacttacgaattgctacagcgatggttctacattgattttggaggagtgtaagtatcatgctaaatctgctgctaaatttt	
		GGCTGCTGCTAATGCTC (244 bp)	
	insertion allele	CCATCTTCCTCCTCCCTTggcagccccgccccccgatttctccatttttttaaagctcgtgtatttcgatcctcaccccagtttggt	
		gtaactttgctgacttacgaattgctacagcgatggttctacattgatttt	
		ggaggagtgtaagtatcatgctaaatctgctgctaaattttGGCTGCTGCTAATGCTC (196 bp)	
	Mut19-N-F	GGAGCTGGTGGTATGGAA	0.5
	Mut19-ins-F	CCATCTTCCTCCTCCCTT	0.5
	Mut19-R	GAGCATTAGCAGCAGCC	0.5
	Mut19-UP	ACCAAACTGGGGTGAGGATCGAAATACACGAGCTTTAAAAAAATG-FITC	
	Mut19-N-DW	LC Red640-AGAAATCACAGATATAATTAGATATTT-P	
	Mut19-ins-DW	LC Red640-AGAAATCGGGGGGCGGGG-P	
G		TCTTAACTAACTCTTTGGTATCAGGTaaatttttaaaatatctaattatatctgtgatttctccatttttttaaagctcg	
		tgtatttcgatcctcaccccagtttggtgtaactttgctgactt**a(a)cg**aattgctacagcga	
		tggttctacattgattttggaggagtgtaagtatcatgctaaatctgctgctaaattttGGCTGCTGCTAATGCTC (217 bp)	
	Mut6-9, 21-F	TCTTAACTAACTCTTTGGTATCAGGT	0.5
	Mut6-9, 21-R	GAGCATTAGCAGCAGCC	0.5
	Mut6-9, 21-UP	TGTATTTCGATCCTCACCCCAGTTTGGTGTAACTT-FITC	
	Mut6-9, 21-DW	LC Red640-GC**G**GACTT**ACG**AATTGCTACAG**C**GA-P	

Upper case and underlined letters indicate the locations of primers and probes, respectively. Inserted DNA is shown in parenthesis. Nucleotides in boldface were used for mutation detection.
F: forward, R: reverse, UP: upstream, DW: downstream, N: normal allele, ins: insertion allele, FITC: fluorescein isothiocyanate, P: phosphate.

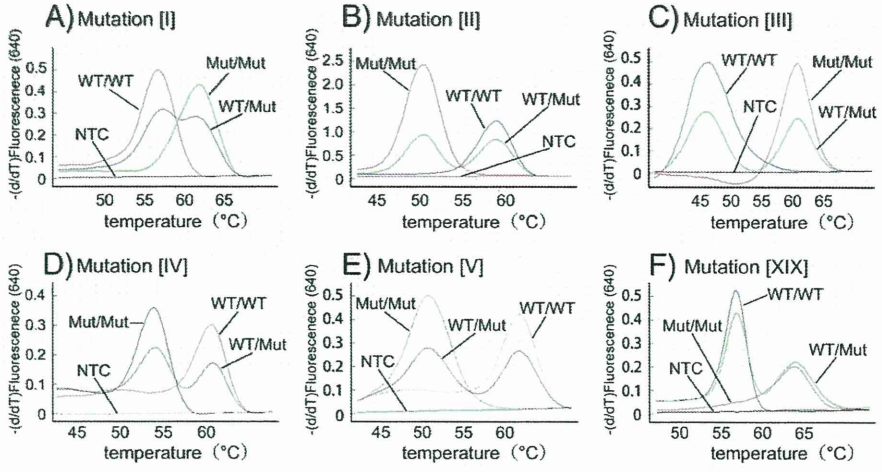

Fig. 2. Typical melting curves used in the detection of mutations [I–V] and [XIX]. Each assay using primer/probe sets A–F is displayed in a separate graph (A–F). WT: wild-type allele, Mut: mutant allele, NTC: no DNA template control.

2.3. Validation of the mutation detection system

After establishing the protocol for detecting the 11 prevalent mutations, 50 DNA samples from patients' blood were sent from Kagoshima University to Tohoku University for the validation of this system in a single-blind manner. Similarly, 26 DNA samples purified from paper-filter blood samples were analyzed in the same manner as the blood DNA samples.

2.4. Estimation of the carrier frequency

For the estimation of the heterozygous carrier frequency, 420 genomic DNA samples from healthy volunteers were screened using the HybProbe analysis for the 11 prevalent mutations. All detected mutations were confirmed by direct sequencing.

2.5. Ethics

This study was approved by the Ethical Committees of Tohoku University School of Medicine and Kagoshima University. Written informed consent was obtained from all participants or their guardians.

3. Results

3.1. Development of the mutation detection system

In primer/probe sets B, D, and E, the reporter probes were designed to be complimentary to the wild-type allele (Fig. 1A). To allow for an improved detection of the mutations, primer/probe sets A and C were designed to be complementary to the mutant allele (Figs. 1B, C). In the primer/probe set F, two forward PCR primers, which were specific to the wild-type and the mutant alleles, were used with a common reverse primer for the co-amplification of the wild-type and 3-kb insertion alleles (Fig. 1E). Two reporter probes, which had a common anchor probe, were used for the detection of the wild-type and mutant alleles. Because the two reporter probes had different melting temperatures, we were able to identify the allele that was amplified. Fig. 2 shows representative results of the melting curve analyses using the primer/probe sets A–F, in which all of the mutant alleles generated distinct peaks corresponding to the wild-type alleles.

In the primer/probe set G, we used a reporter probe that was complementary to the mutant [XXI] allele (Fig. 1D). All five mutations in exon 17 were successfully differentiated from the wild-type allele (Figs. 3A–E). The [XXIX] mutation is an additional mutation in exon

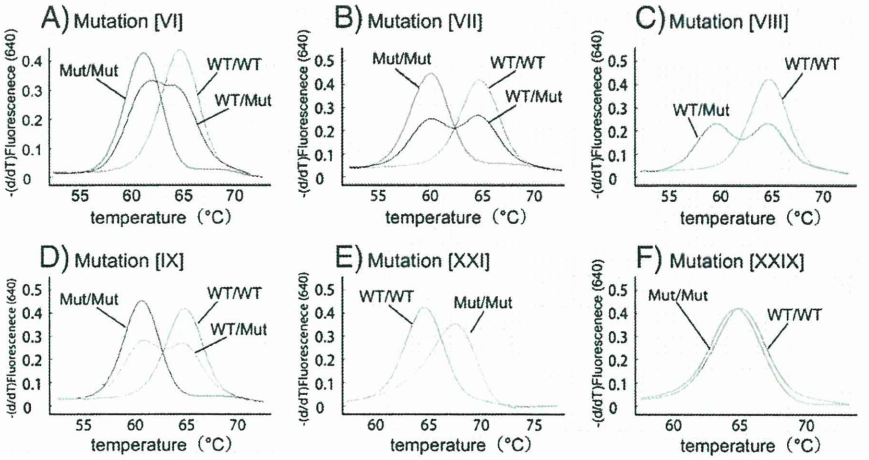

Fig. 3. Typical melting curves used in the detection of mutations [VI–XI], [XXI], and [XXIX] on exon 17. Genotyping was performed using primer/probe set G. Each melting curve for a target mutation is displayed in a separate graph (A–F). Note that mutation [XXIX] (F) is a non-target mutation on the anchor probe. WT: wild-type allele, Mut: mutant allele.

17 that is not listed in Table 1. The [XXIX] mutation is located in the anchor-probe binding site and not on the reporter-probe binding site (Fig. 1D). To examine the effect of mutations on the anchor probe, we genotyped a patient with a heterozygous [XXIX] mutation using primer/probe set G (Fig. 3F). We found no change in the melting curves between the wild-type allele and the [XXIX] allele, thereby suggesting that point mutations within the anchor probe sequence have little effect on the melting curve analysis.

3.2. Validation

The genotypes determined at Tohoku University using the proposed method and those determined at Kagoshima University using a previously published method were identical for the 11 common mutations (Table S1 in supplementary material). We performed a similar test using DNA samples purified from filter-paper blood samples to determine if this method could be used for newborn screening. The genotypes determined in both laboratories were identical for all 26 DNA samples (Table S2 in supplementary material).

3.3. Frequency of eleven prevalent mutations

We found four heterozygous carriers of mutation [I], three of mutation [II], and two of mutation [V]. In addition, primer/probe set G detected one heterozygous mutation, which was confirmed as mutation [VIII] by direct sequencing. Altogether, 10 mutations were detected in 420 Japanese healthy controls.

4. Discussion

We developed a simple and rapid genetic test using real-time PCR combined with the HybProbe system for the 11 prevalent mutations in *SLC25A13*: mutations [I], [II], [III], [IV], [V], [VI], [VII], [VIII], [IX], [XIX], and [XXI]. This genetic test is a closed-tube assay in which no post-PCR handling of the samples is required. In addition, the genotyping is completed within 1 h. This test can utilize DNA samples purified from both peripheral blood and filter-paper blood. The reliability of the test was confirmed by genotyping 76 blind DNA samples from patients with citrin deficiency, including 50 peripheral blood and 26 filter-paper blood DNA samples. Because screening for the 11 targeted mutations would identify 95% of mutant alleles in the Japanese population [19], both, one, and no mutant alleles are expected to be identified in 90.4%, 9.3%, and less than 0.3% of patients, respectively. This genetic test would be useful not only in Japan but also other East Asian countries, including China, Korea, Taiwan and Vietnam, in which the same mutations are prevalent. Our test is expected to detect 76–87% of the mutant alleles in the Chinese population [12,19,25], 95–100% in the Korean population [12,19,26], 60–68% in the Taiwanese population [27,28], and 100% in the Vietnamese population [12,19]. If we were to prepare a primer/probe set for mutation [X]:g.IVS6+5G>A [12], which is prevalent in Taiwan, the estimated sensitivity would exceed 90% in the Taiwanese population [27,28].

Recently, the high resolution melting (HRM) method was reported to be suitable for the screening of mutations in the diagnosis of citrin deficiency [28]. HRM analysis is a closed-tube assay that screens for any base changes in the amplicons. The presence of SNPs anywhere on the amplicons can affect the melting curve, thereby suggesting that HRM is not suitable for screening for known mutations, but rather, is best suited to screening for unknown mutations. When we detected one heterozygous prevalent mutation, we performed HRM screening for all 17 exons of *SLC25A13*. After HRM screening, only the HRM-positive exons were subjected to direct sequencing analysis. Several mutant alleles were identified using this approach.

The frequency of homozygotes, including compound heterozygotes, presenting *SLC25A13* mutations in the population at Kagoshima (a prefecture in the southern part of Japan) has been calculated to be 1/17,000 based on the carrier rate (1/65) [19]. The prevalence of NICCD has been also reported to be 1/17,000–34,000 [29]. In this study, the carrier rate in Miyagi (a prefecture in northern Japan) was 1/42 (95% confidential interval, 1/108–1/26), thereby yielding an estimated frequency of patients with citrin deficiency of 1/7,100. Our result, together with the previous report [19], suggests that a substantial fraction of the homozygotes or compound heterozygotes of SLC25A13 mutations was asymptomatic during the neonatal period.

The early and definitive diagnosis of citrin deficiency may be beneficial for patients with citrin deficiency by encouraging specific dietary habits and avoiding iatrogenic worsening of brain edema by glycerol infusion when patients develop encephalopathy [30,31]. Because the screening of blood citrulline levels by tandem mass analysis at birth does not detect all patients with citrin deficiency, the development of a genetic test would be welcomed. In this study, we demonstrated that genomic DNA extracted from filter paper blood samples was correctly genotyped, thereby indicating the feasibility of newborn screening using this genetic test. If 100,000 babies in the northern part of Japan were screened by this method, we would detect 14 homozygotes or compound heterozygotes with *SLC25A13* mutations and 2400 heterozygous carriers. In 2400 heterozygous carriers, we would expect to observe only 1 to 2 compound heterozygotes with one target and one non-target mutation. The estimated frequency of babies with two non-target mutations is 0.04/100,000. Our genetic method would therefore allow us to screen newborn babies efficiently. If we performed this genetic test in a high-throughput real-time PCR system, such as a 384- or 1,536-well format, the cost per sample could be lowered.

In conclusion, we have established a rapid and simple detection system using the HybProbe assay for the 11 prevalent mutations in *SLC25A13*. This system could be used to screen newborns for citrin deficiency and may facilitate the genetic diagnosis of citrin deficiency, especially in East Asian populations.

Supplementary materials related to this article can be found online at doi:10.1016/j.ymgme.2011.12.024.

Acknowledgments

The authors acknowledge the contribution of Dr. Keiko Kobayashi, who passed away on December 21th, 2010. Dr. Kobayashi discovered that the *SLC25A13* gene is responsible for citrin deficiency and devoted much of her life to elucidating the mechanism of citrin deficiency. This work was supported by grants from the Ministry of Education, Culture, Sports, Science, and Technology and the Ministry of Health, Labor, and Public Welfare.

References

[1] K. Kobayashi, D.S. Sinasac, M. Iijima, A.P. Boright, L. Begum, J.R. Lee, T. Yasuda, S. Ikeda, R. Hirano, H. Terazono, M.A. Crackower, I. Kondo, L.C. Tsui, S.W. Scherer, T. Saheki, The gene mutated in adult-onset type II citrullinaemia encodes a putative mitochondrial carrier protein, Nat. Genet. 22 (1999) 159–163.
[2] T. Ohura, K. Kobayashi, Y. Tazawa, I. Nishi, D. Abukawa, O. Sakamoto, K. Iinuma, T. Saheki, Neonatal presentation of adult-onset type II citrullinemia, Hum. Genet. 108 (2001) 87–90.
[3] Y. Tazawa, K. Kobayashi, T. Ohura, D. Abukawa, F. Nishinomiya, Y. Hosoda, M. Yamashita, I. Nagata, Y. Kono, T. Yasuda, N. Yamaguchi, T. Saheki, Infantile cholestatic jaundice associated with adult-onset type II citrullinemia, J. Pediatr. 138 (2001) 735–740.
[4] T. Tomomasa, K. Kobayashi, H. Kaneko, H. Shimura, T. Fukusato, M. Tabata, Y. Inoue, S. Ohwada, M. Kasahara, Y. Morishita, M. Kimura, T. Saheki, A. Morikawa, Possible clinical and histologic manifestations of adult-onset type II citrullinemia in early infancy, J. Pediatr. 138 (2001) 741–743.
[5] T. Shigeta, M. Kasahara, T. Kimura, A. Fukuda, K. Sasaki, K. Arai, A. Nakagawa, S. Nakagawa, K. Kobayashi, S. Soneda, H. Kitagawa, Liver transplantation for an

infant with neonatal intrahepatic cholestasis caused by citrin deficiency using heterozygote living donor, Pediatr. Transplant. 14 (2009) E86–88.
[6] M. Kasahara, S. Ohwada, T. Takeichi, H. Kaneko, T. Tomomasa, A. Morikawa, K. Yonemura, K. Asonuma, K. Tanaka, K. Kobayashi, T. Saheki, I. Takeyoshi, Y. Morishita, Living-related liver transplantation for type II citrullinemia using a graft from heterozygote donor, Transplantation 71 (2001) 157–159.
[7] Y. Takashima, M. Koide, H. Fukunaga, M. Iwai, M. Miura, R. Yoneda, T. Fukuda, K. Kobayashi, T. Saheki, Recovery from marked altered consciousness in a patient with adult-onset type II citrullinemia diagnosed by DNA analysis and treated with a living related partial liver transplantation, Intern. Med. 41 (2002) 555–560.
[8] A. Tamamori, Y. Okano, H. Ozaki, A. Fujimoto, M. Kajiwara, K. Fukuda, K. Kobayashi, T. Saheki, Y. Tagami, T. Yamano, Neonatal intrahepatic cholestasis caused by citrin deficiency: severe hepatic dysfunction in an infant requiring liver transplantation, Eur. J. Pediatr. 161 (2002) 609–613.
[9] T. Ohura, K. Kobayashi, Y. Tazawa, D. Abukawa, O. Sakamoto, S. Tsuchiya, T. Saheki, Clinical pictures of 75 patients with neonatal intrahepatic cholestasis caused by citrin deficiency (NICCD), J. Inherit. Metab. Dis. 30 (2007) 139–144.
[10] T. Yasuda, N. Yamaguchi, K. Kobayashi, I. Nishi, H. Horinouchi, M.A. Jalil, M.X. Li, M. Ushikai, M. Iijima, I. Kondo, T. Saheki, Identification of two novel mutations in the SLC25A13 gene and detection of seven mutations in 102 patients with adult-onset type II citrullinemia, Hum. Genet. 107 (2000) 537–545.
[11] N. Yamaguchi, K. Kobayashi, T. Yasuda, I. Nishi, M. Iijima, M. Nakagawa, M. Osame, I. Kondo, T. Saheki, Screening of SLC25A13 mutations in early and late onset patients with citrin deficiency and in the Japanese population: identification of two novel mutations and establishment of multiple DNA diagnosis methods for nine mutations, Hum. Mutat. 19 (2002) 122–130.
[12] Y.B. Lu, K. Kobayashi, M. Ushikai, A. Tabata, M. Iijima, M.X. Li, L. Lei, K. Kawabe, S. Taura, Y. Yang, T.-T. Liu, S.-H. Chiang, K.-J. Hsiao, Y.-L. Lau, L.-C. Tsui, D.H. Lee, T. Saheki, Frequency and distribution in East Asia of 12 mutations identified in the SLC25A13 gene of Japanese patients with citrin deficiency, J. Hum. Genet. 50 (2005) 338–346.
[13] E. Ben-Shalom, K. Kobayashi, A. Shaag, T. Yasuda, H.-Z. Gao, T. Saheki, C. Bachmann, O. Elpeleg, Infantile citrullinemia caused by citrin deficiency with increased dibasic amino acids, Mol. Genet. Metab. 77 (2002) 202–208.
[14] J. Takaya, K. Kobayashi, A. Ohashi, M. Ushikai, A. Tabata, S. Fujimoto, F. Yamato, T. Saheki, Y. Kobayashi, Variant clinical courses of 2 patients with neonatal intrahepatic cholestasis who have a novel mutation of SLC25A13, Metab. Clin. Exp. 54 (2005) 1615–1619.
[15] A. Luder, A. Tabata, M. Iijima, K. Kobayashi, H. Mandel, Citrullinaemia type 2 outside East Asia: Israeli experience, J. Inherit. Metab. Dis. 29 (2006) 59.
[16] T. Hutchin, M. Preece, K. Kobayashi, T. Saheki, R. Brown, D. Kelly, P. McKiernan, A. Green, U. Baumann, Neonatal intrahepatic cholestasis caused by citirn deficiency (NICCD) in a European patient, J. Inherit. Metab. Dis. 29 (2006) 112.
[17] J.-S. Sheng, M. Ushikai, M. Iijima, S. Packman, K. Weisiger, M. Martin, M. McCracken, T. Saheki, K. Kobayashi, Identification of a novel mutation in a Taiwanese patient with citrin deficiency, J. Inherit. Metab. Dis. 29 (2006) 163.
[18] J.M. Ko, G.-H. Kim, J.-H. Kim, J.Y. Kim, J.-H. Choi, M. Ushikai, T. Saheki, K. Kobayashi, H.-W. Yoo, Six cases of citrin deficiency in Korea, Int. J. Mol. Med. 20 (2007) 809–815.
[19] A. Tabata, J.-S. Sheng, M. Ushikai, Y.-Z. Song, H.-Z. Gao, Y.-B. Lu, F. Okumura, M. Iijima, K. Mutoh, S. Kishida, T. Saheki, K. Kobayashi, Identification of 13 novel mutations including a retrotransposal insertion in SLC25A13 gene and frequency of 30 mutations found in patients with citrin deficiency, J. Hum. Genet. 53 (2008) 534–545.
[20] P.S. Bernard, R.S. Ajioka, J.P. Kushner, C.T. Wittwer, Homogeneous multiplex genotyping of hemochromatosis mutations with fluorescent hybridization probes, Am. J. Pathol. 153 (1998) 1055–1061.
[21] C.N. Gundry, P.S. Bernard, M.G. Herrmann, G.H. Reed, C.T. Wittwer, Rapid F508del and F508C assay using fluorescent hybridization probes, Genet. Test. 3 (1999) 365–370.
[22] T. Saheki, K. Kobayashi, I. Inoue, Hereditary disorders of the urea cycle in man: biochemical and molecular approaches, Rev. Physiol. Biochem. Pharmacol. 108 (1987) 21–68.
[23] K. Kobayashi, M. Horiuchi, T. Saheki, Pancreatic secretory trypsin inhibitor as a diagnostic marker for adult-onset type II citrullinemia, Hepatology 25 (1997) 1160–1165.
[24] Y. Tazawa, K. Kobayashi, D. Abukawa, I. Nagata, S. Maisawa, R. Sumazaki, T. Iizuka, Y. Hosoda, M. Okamoto, J. Murakami, S. Kaji, A. Tabata, Y.B. Lu, O. Sakamoto, A. Matsui, S. Kanzaki, G. Takada, T. Saheki, K. Iinuma, T. Ohura, Clinical heterogeneity of neonatal intrahepatic cholestasis caused by citrin deficiency: case reports from 16 patients, Mol. Genet. Metab. 83 (2004) 213–219.
[25] H.Y. Fu, S.R. Zhang, X.H. Wang, T. Saheki, K. Kobayashi, J.S. Wang, The mutation spectrum of the SLC25A13 gene in Chinese infants with intrahepatic cholestasis and aminoacidemia, J. Gastroenterol. 46 (2011) 510–518.
[26] K. Kobayashi, Y.B. Lu, M.X. Li, I. Nishi, K.-J. Hsiao, K. Choeh, Y. Yang, W.-L. Hwu, J.K.V. Reichardt, F. Palmieri, Y. Okano, T. Saheki, Screening of nine SLC25A13 mutations: their frequency in patients with citrin deficiency and high carrier rates in Asian populations, Mol. Genet. Metab. 80 (2003) 356–359.
[27] T. Saheki, K. Kobayashi, M. Iijima, M. Horiuchi, L. Begum, M.A. Jalil, M.X. Li, Y.B. Lu, M. Ushikai, A. Tabata, M. Moriyama, K.-J. Hsiao, Y. Yang, Adult-onset type II citrullinemia and idiopathic neonatal hepatitis caused by citrin deficiency: involvement of the aspartate glutamate carrier for urea synthesis and maintenance of the urea cycle, Mol. Genet. Metab. 81 (Suppl 1) (2004) S20–S26.
[28] J.T. Lin, K.J. Hsiao, C.Y. Chen, C.C. Wu, S.J. Lin, Y.Y. Chou, S.C. Shiesh, High resolution melting analysis for the detection of SLC25A13 gene mutations in Taiwan, Clin. Chim. Acta 412 (2011) 460–465.
[29] Y. Shigematsu, S. Hirano, I. Hata, Y. Tanaka, M. Sudo, N. Sakura, T. Tajima, S. Yamaguchi, Newborn mass screening and selective screening using electrospray tandem mass spectrometry in Japan, J. Chromatogr. B Analyt. Technol. Biomed. Life Sci. 776 (2002) 39–48.
[30] M. Yazaki, Y.-i. Takei, K. Kobayashi, T. Saheki, S.-I. Ikeda, Risk of worsened encephalopathy after intravenous glycerol therapy in patients with adult-onset type II citrullinemia (CTLN2), Intern. Med. 44 (2005) 188–195.
[31] H. Takahashi, T. Kagawa, K. Kobayashi, H. Hirabayashi, M. Yui, L. Begum, T. Mine, S. Takagi, T. Saheki, Y. Shinohara, A case of adult-onset type II citrullinemia—deterioration of clinical course after infusion of hyperosmotic and high sugar solutions, Med. Sci. Monit. 12 (2006) CS13–CS15.

Homozygous c.14576G>A variant of *RNF213* predicts early-onset and severe form of moyamoya disease

S. Miyatake, MD
N. Miyake, MD, PhD
H. Touho, MD, PhD
A. Nishimura-Tadaki, PhD
Y. Kondo, MD
I. Okada, MD
Y. Tsurusaki, PhD
H. Doi, MD, PhD
H. Sakai, PhD
H. Saitsu, MD, PhD
K. Shimojima, MD
T. Yamamoto, MD, PhD
M. Higurashi, MD
N. Kawahara, MD, PhD
H. Kawauchi, MD
K. Nagasaka, MD, PhD
N. Okamoto, MD
T. Mori, MD, PhD
S. Koyano, MD, PhD
Y. Kuroiwa, MD, PhD
M. Taguri, PhD
S. Morita, PhD
Y. Matsubara, MD, PhD
S. Kure, MD, PhD
N. Matsumoto, MD, PhD

Correspondence & reprint requests to Dr. Matsumoto: naomat@yokohama-cu.ac.jp

ABSTRACT

Objective: *RNF213* was recently reported as a susceptibility gene for moyamoya disease (MMD). Our aim was to clarify the correlation between the *RNF213* genotype and MMD phenotype.

Methods: The entire coding region of the *RNF213* gene was sequenced in 204 patients with MMD, and corresponding variants were checked in 62 pairs of parents, 13 mothers and 4 fathers of the patients, and 283 normal controls. Clinical information was collected. Genotype-phenotype correlations were statistically analyzed.

Results: The c.14576G>A variant was identified in 95.1% of patients with familial MMD, 79.2% of patients with sporadic MMD, and 1.8% of controls, thus confirming its association with MMD, with an odds ratio of 259 and $p < 0.001$ for either heterozygotes or homozygotes. Homozygous c.14576G>A was observed in 15 patients but not in the controls and unaffected parents. The incidence rate for homozygotes was calculated to be >78%. Homozygotes had a significantly earlier age at onset compared with heterozygotes or wild types (median age at onset 3, 7, and 8 years, respectively). Of homozygotes, 60% were diagnosed with MMD before age 4, and all had infarctions as the first symptom. Infarctions at initial presentation and involvement of posterior cerebral arteries, both known as poor prognostic factors for MMD, were of significantly higher frequency in homozygotes than in heterozygotes and wild types. Variants other than c.14576G>A were not associated with clinical phenotypes.

Conclusions: The homozygous c.14576G>A variant in *RNF213* could be a good DNA biomarker for predicting the severe type of MMD, for which early medical/surgical intervention is recommended, and may provide a better monitoring and prevention strategy. **Neurology® 2012;78:803-810**

GLOSSARY

CI = confidence interval; **HRM** = high-resolution melting; **MMD** = moyamoya disease; **OR** = odds ratio; **PCA** = posterior cerebral artery.

Moyamoya disease (MMD) is a cerebrovascular disease, which is now a relatively common cause of pediatric strokes.[1,2] Annual incidence is estimated to be 0.35–0.54 per 100,000 person-years in Japan[3,4] and about one tenth of that in Europe.[5,6] MMD can lead to devastating neurologic deficits and intellectual impairments if left untreated.

Although MMD is a progressive disease, its natural history varies from slow progression to rapid neurologic decline.[7] Preoperative infarctions, early age at onset, intellectual impairment, seizure, and progressive posterior cerebral artery (PCA) stenosis are known prognostic factors.[8–11] Surgical revascularization can improve the cerebrovascular hemodynamics and prevent subsequent attacks in the ischemic type of MMD.[8] Thus, early diagnosis and surgical intervention are very important.

Genetic factors underlying MMD are of clinical relevance. Epidemiologic studies have shown that about 15% of patients had a family history.[12] Anticipation of the disease is

Supplemental data at www.neurology.org

Supplemental Data

From the Department of Human Genetics (S.M., N.M., A.N.-T., Y.K., I.O., Y.T., H.D., H.Sakai, H.Saitsu, N.M.), Yokohama City University Graduate School of Medicine, Yokohama; Touho Neurosurgical Clinic (H.T.), Osaka; Tokyo Women's Medical University Institute for Integrated Medical Sciences (K.S., T.Y.), Tokyo; Department of Neurosurgery (M.H., N.K.), Yokohama City University Graduate School of Medicine, Yokohama; Department of Neurosurgery (H.K., K.N.), Tone Chuo Hospital, Gunma; Division of Medical Genetics (N.O.), Osaka Medical Center and Research Institute for Maternal and Child Health, Osaka; Department of Rehabilitation Medicine (T.M.), Ichikawa City Rehabilitation Hospital, Ichikawa; Department of Clinical Neurology and Stroke Medicine (S.K., Y.K.), Yokohama City University Graduate School of Medicine, Yokohama; Department of Biostatistics and Epidemiology (M.T., S.M.), Yokohama City University Medical Center, Yokohama; Department of Medical Genetics (Y.M.), Tohoku University School of Medicine, Sendai; Department of Pediatrics (S.K.), Tohoku University School of Medicine, Sendai, Japan.

Disclosure: Author disclosures are provided at the end of the article.

Table 1 Sample demographics of patients with moyamoya disease and controls[a]

Clinical features	No. of patients (%)	No. of patients without data
MMD	204	
Gender (M/F)	68 (33.5)/135 (66.5)	1
Distribution of age at onset	0–58 y	7
Frequency of childhood onset (<15 y)	143 (72.6)	
Frequency of childhood onset (<4 y)	36 (18.3)	
Clinical manifestation		11
Infarction	87 (45.1)	
TIA	77 (39.9)	
ICH/IVH	17 (8.8)	
Others	12 (6.2)	
With family history	41 (20.1)	0
With intellectual impairment	33 (17.7)	18
With epilepsy	33 (17.6)	16
PCA involvement		52
Unilateral	31 (20.4)	
Bilateral	43 (28.3)	
Total	74 (48.7)	
Bilateral MMD	148 (96.1)	50
Controls	283	
Gender (M/F)	140 (51.5):132 (48.5)	11

Abbreviations: ICH/IVH = intracranial hemorrhage/intraventricular hemorrhage; MMD = moyamoya disease; PCA = posterior cerebral artery; TIA = transient ischemic attack.
[a] Numbers of patients (%) in each feature are shown, except for the distribution of ages at onset for all patients.

also observed in familial MMD.[13] Recently, the important MMD susceptibility gene, *RNF213*, was identified.[14,15] However, its clinical relevance remains unknown. For this investigation, we conducted a comprehensive genetic study of *RNF213* as well as a clinical phenotype analysis of MMD.

METHODS

Study subjects. Blood samples from 204 Japanese patients with MMD were obtained consecutively between January 2008 and February 2011. There were no sample overlaps between ours and those in the previous studies.[14,15] MMD was diagnosed as either definite (bilateral) or probable (unilateral) according to published guidelines.[16] Six patients with probable MMD were female adults and 5 of them had sporadic MMD. The medical charts were completed by the clinicians who were blinded to the genotype of the patients. Sample demographics are shown in table 1. We also obtained either blood or saliva samples from 62 pairs of parents, as well as 4 fathers and 13 mothers whose partners were unavailable. As many as 94 to 283 samples from healthy Japanese individuals were tested as normal controls for each sequence variant found.

Standard protocol approvals, registrations, and patient consents. Experimental protocols were approved by the Committee for Ethical Issue at Yokohama City University School of Medicine. Written informed consents were obtained from all the patients or their parents.

Mutation screening. Genomic DNA was obtained from peripheral blood leukocytes using QuickGene-610L (Fujifilm, Tokyo, Japan) or from saliva using Oragene DNA (DNA Genotek, Kanata, Canada). DNA was amplified using GenomiPhi version 2 (GE Healthcare, Buckinghamshire, UK). Mutation analysis of exons and exon-intron borders covering the coding region of *RNF213* (GenBank accession number, NM_020914.4), except for exon 61, was performed in all MMD patient samples by high-resolution melting (HRM) analysis on a LightCycler 480 System II (Roche Diagnostics, Basel, Switzerland). Primer sequences, PCR conditions, and HRM settings are available on request. HRM analysis with and without the spike-in method was performed for the detection of homozygous mutations.[17] If samples showed any aberrant melting curve patterns, direct sequencing was performed using an ABI Genetic Analyzer 3100 or 3500xL (Applied Biosystems, Foster City, CA) and analyzed with sequence analysis software version 5.1.1 (Applied Biosystems) and Sequencher 4.10 build 5828 (GeneCodes Corporation, Ann Arbor, MI). For exon 61, which bears the c.14576G>A variant, direct sequencing was performed for all patients with MMD and their parental samples. Additional screenings by HRM analysis were performed for the confirmed mutations in up to 283 normal control Japanese individuals. All variants were confirmed with PCR direct sequencing using either genomic DNA or another DNA, amplified with GenomiPhi separately. No discrepancy was seen in the data between the 2 different conditions of DNA.

Statistical analysis. Patients without information for each clinical feature (listed below) were excluded from the analyses (table 1 and tables e-2 and e-3 on the *Neurology*® Web site at www.neurology.org). All statistical analyses were performed using SPSS Statistics 19 (IBM, New York, NY) software. χ^2 tests were applied to compare each categorical phenotype variable between different genotypes: clinical symptom at onset, with/without family history, intellectual impairment, epilepsy, and the unilateral/bilateral distribution of vasculopathy. Non-normally distributed continuous variables, such as age at onset and the number of steno-occlusive PCA arteries were compared using the Mann-Whitney *U* test and Kruskal-Wallis test between different genotypes. $p < 0.05$ was considered statistically significant. A Kaplan-Meier curve was used to assess the cumulative incidence with the log-rank test. The Cox regression model was used to test which variables were associated with age at onset. The exact 95% confidence interval (CI) of the incidence rate of MMD was calculated according to the binomial distribution. The comparisons of clinical features between parent-offspring pairs or sibling pairs were performed using the Wilcoxon signed-rank test and McNemar test.

RESULTS

Identification of *RNF213* variants. c.14576G>A was identified in 39 of 41 patients with familial MMD (95.1%), in 129 of 163 patients with nonfamilial MMD (79.2%), and in 5 of

Table 2 Distribution of the c.14576G>A variant among patients with MMD, parents of the patients, and normal control Japanese individuals[a]

		c.14576G>A genotype			
	Total	Wild-type: G/G (%)	Heterozygous: G/A (%)	Homozygous: A/A (%)	GA + A/A (%)
Patients with MMD	204	36 (17.6)	153 (75.0)	15 (7.4)	168 (82.4)
Sporadic	163	34 (20.8)	117 (71.8)	12 (7.4)	129 (79.2)
With no other variant	137	20 (14.6)	105 (76.6)	12 (8.8)	117 (85.4)
With one other variant	25	13 (52)	12 (48)	0	12 (48)
With one other homozygous variants	1	1 (100)	0	0	0
Familial	41	2 (4.9)	36 (87.8)	3 (7.3)	39 (95.1)
With no other variant	36	0	33 (91.7)	3 (8.3)	36 (100)
With one other variant	3	0	3 (100)	0	3 (100)
With 2 other compound heterozygous variants	2	2 (100)	0	0	0
Parents of patients with MMD	141	77 (54.6)	63 (44.7)	1 (0.7)	64 (45.4)
Affected	9	0	8 (88.9)	1 (11.1)	9 (100)
Unaffected	132	77 (58.3)	55 (41.7)	0	55 (41.7)
Normal controls	283	278 (98.2)	5 (1.8)	0	5 (1.8)
OR (patients with MMD vs normal control)			236	ND	259
95% CI			91–615		100–674
p (Fisher exact test)			<0.001	<0.001	<0.001

Abbreviations: CI = confidence interval; MMD = moyamoya disease; ND = not determined; OR = odds ratio.
[a] Numbers of patients in each category (%) are shown.

283 normal control Japanese individuals (1.8%) (table 2 and table e-1). Sixty-two pairs of parents were also tested for the c.14576G>A genotype, with the conclusion that the c.14576G>A variant allele was inherited from either or both parents in all patients tested. Among 168 patients with the c.14576G>A variant, 15 had a homozygous change, whereas none of the controls and unaffected parents did. We conclude that the heterozygous c.14576G>A variant increases the risk for MMD with an odds ratio (OR) of 236 (95% CI 91–615, $p < 0.001$). Because no homozygous mutation was detected in the control samples or unaffected family members, the OR for the homozygote could not be calculated (∞), suggesting its strong effect. The incidence rate of MMD was calculated to be extremely high with a 95% CI of 0.78–1.00 with the homozygous mutation. Eighteen other genetic variants beside c.14576G>A were also identified in *RNF213* (figure 1, table e-1). Sixteen of them were novel, which had not been reported in the previous studies.[14,15] Two of the variants were also found in the previous study[14]; however, they were thought to be common single nucleotide polymorphisms because they were also found in the normal controls without the significant difference of frequency. Other genetic variants showed a relatively small OR without any significance (table e-1). Thirty-one patients had these individual variants (table 2). Fifteen of them also had the heterozygous c.14576G>A, and 4 of 5 patients whose parents' samples were available had these 2 variants existing as compound heterozygotes (for example, one variant from the father and the other from the mother). In the other 16 patients having no c.14576G>A, 1 had a homozygous c.13342G>A variant, and 2 had 2 variants: c.13342G>A and c.14053G>A as a compound heterozygote. Of the novel 16 variants, 11 of them were not found in 188 normal control Japanese individuals and were all private mutations (only once in one family).

Correlation between the c.14576G>A genotype and clinical phenotype. We compared the clinical features of patients with MMD according to the c.14576G>A genotype, the wild type (genotype GG, as group GG), the heterozygote (genotype GA, as group GA), or the mutant homozygote (genotype AA, as group AA). Age at onset was lower in AA than in GA or GG ($p = 0.002$ or $p = 0.007$) (figure 2A and table e-2). Median age at onset was 3 years in AA, 7 years in GA, and 8 years in GG. Among those with childhood onset (age at onset <15 years), in whom the effect of secondary vascular changes in later life could be ignored and therefore a pure genetic effect could be expected, the association between earlier onset age and the homozygous c.14576G>A genotype was clearly replicated (table e-2). Although the clinical manifestation is different

Figure 1 Schematic diagram of the RNF213 protein and genomic structure of *RNF213*

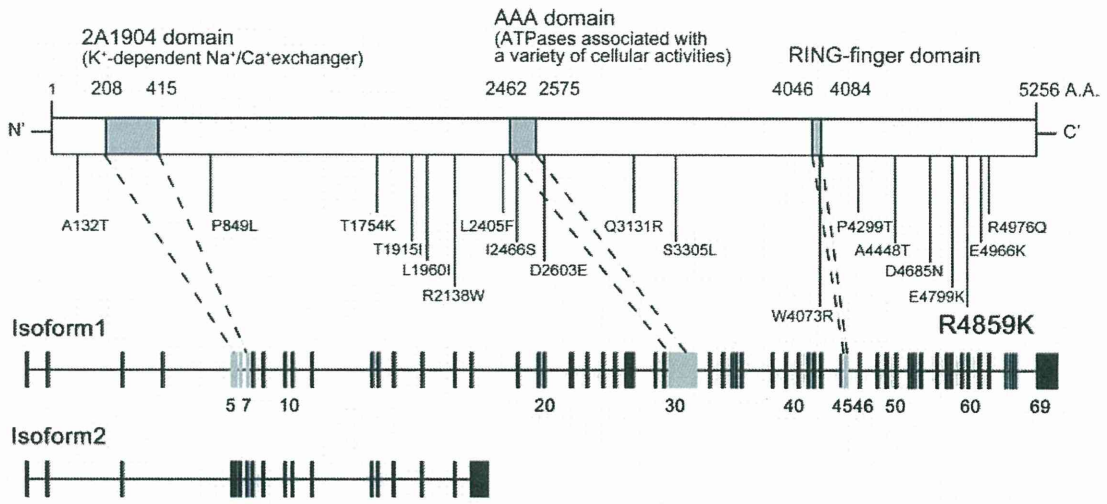

A schematic presentation of the RNF213 protein with 3 conserved domains, the genetic variants we have identified, and the genomic structures of 2 *RNF213* isoforms (shown from top to bottom). All missense changes, including R4859K (c.14576G>A as larger characters) are indicated. A.A. = amino acids; AAA = ATPases associated with a variety of cellular activities; RING = really interesting new gene. (Based on National Center for Biotechnology Information Reference sequence, NP_065965.4.)

between the childhood-onset group and the adult-onset group, the rates of the patients with this variant, 83.2% (119 of 143 patients) and 79.6% (43 of 54 patients), respectively, were not significantly different. Among adult patients, there was no significant difference in the rate of having this variant between those with familial history (84.6%, 11 of 13 patients) and those without (78.0%, 32 of 41 patients). The univariate Cox regression analysis showed that only the c.14576G>A genotype was the significant predictive variable for age at onset (table e-4). The cumulative incidence of MMD was higher in AA than GA or GG at almost all age distributions (figure 2B), but this tendency was more apparent in the childhood-onset group. Further investigation with more AA and GG patients is necessary for better statistical accuracy. More AA patients were affected before age 4, compared with GA and GG patients ($p < 0.001$) (figure 3A). All AA patients had infarctions at initial presentation.

Figure 2 Correlation between the c.14576G>A variant and age at onset

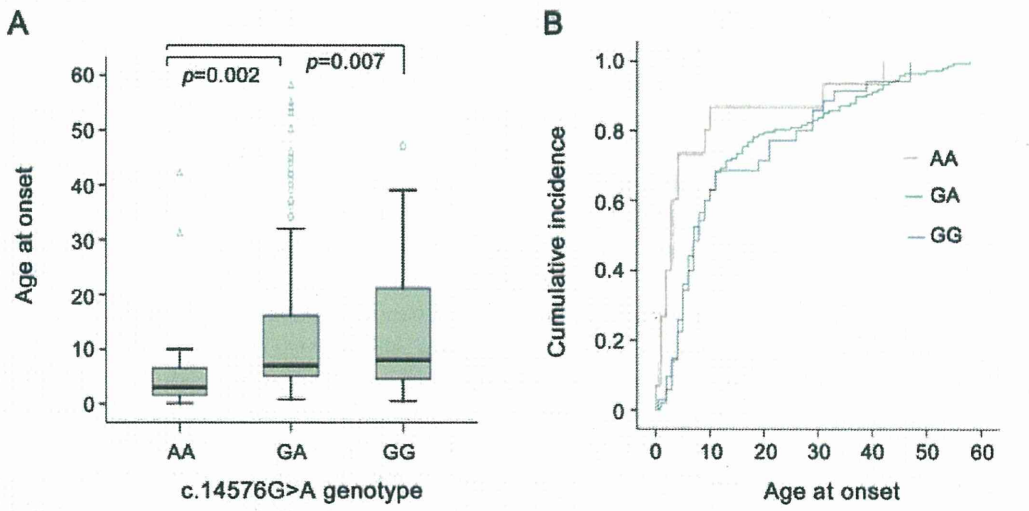

(A) A box plot of age at onset between 3 groups of patients with either the mutant homozygote (AA), heterozygote (GA), or wild type (GG) of the c.14576G>A variant. ○ indicates mild outliers; △ indicates extreme outliners. (B) Cumulative incidence curve of the 3 groups of patients with either the mutant homozygote (AA), heterozygote (GA), or wild type (GG) of the c.14576G>A variant.

Figure 3 Correlation between c.14576G>A variant and clinical features

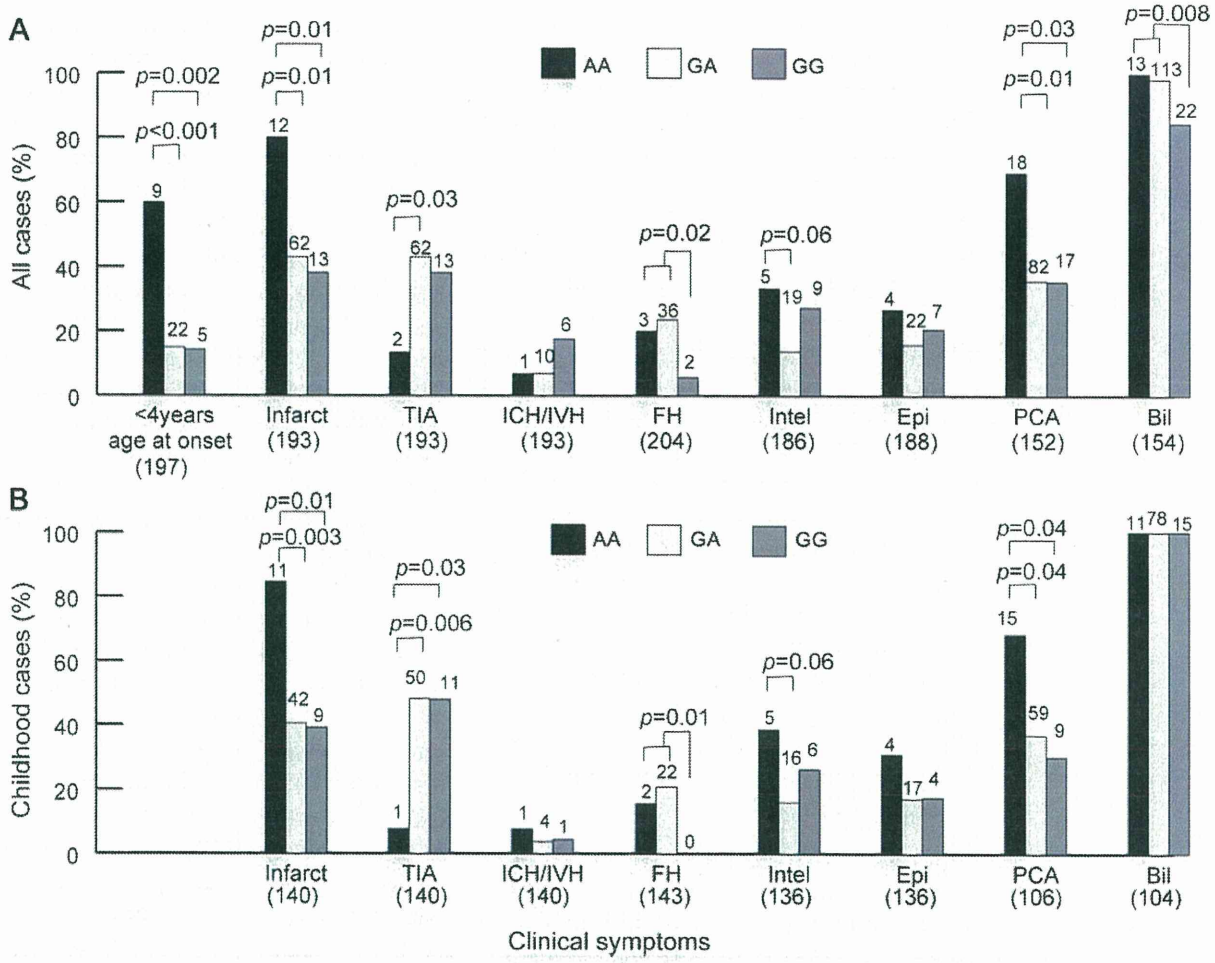

(A) The clinical characteristics of MMD for the 3 groups of patients with either the mutant homozygote (AA), heterozygote (GA), or wild type (GG) of the c.14576G>A variant (204 patients). The numbers of total patients with clinical records regarding either the presence or absence of each characteristic are indicated below the bars, and the numbers of patients in each group are indicated above the respective bars. (B) Clinical characteristics of MMD for the 3 groups of patients with either the mutant homozygote (AA), heterozygote (GA), or wild type (GG) of the c.14576G>A variant among those with age at onset younger than 15 years. The numbers of total patients with clinical records regarding either the presence or absence of each characteristic are indicated below the bars, and the numbers of patients in each group are indicated above the respective bars. Bil = bilateral vasculopathy; Epi = epilepsy; FH = with family history; ICH/IVH = intracranial hemorrhage/intraventricular hemorrhage, Infarct = infarction; Intel = intellectual impairment; PCA = posterior cerebral artery involvement.

The frequencies of other clinical features of MMD in AA, GA, and GG were also compared (figure 3A and table e-2). As the clinical manifestation at diagnosis, infarction was more common in AA than in GA or GG ($p = 0.01$, OR 5.3, 95% CI 1.43–19.56 or $p = 0.01$, OR 6.5, 95%CI 1.53–27.32); TIA was less common in AA than in GA ($p = 0.03$; OR 0.20; 95% CI 0.04–0.94). Bilateral MMD and family history of the disease were more frequent in AA and GA than in GG ($p = 0.008$, OR 11, 95% CI 1.98–66.36 and $p = 0.02$, OR 5.1, 95% CI 1.18–22.36). The number of steno-occlusive PCAs was larger in AA than in GA ($p = 0.01$) (counted as 2 arteries per person). Seventy-four of the 152 patients (48.6%) had PCA lesions, and infarctions and intellectual impairment were more frequent in those with PCA involvement than those without (infarctions 68.9% vs 30.8%, $p < 0.001$; intellectual impairment 26.8% vs 5.3%, $p < 0.001$). Intellectual impairment and epilepsy tended to be a more common complication in AA than in GA, with and without marginal significance. We also compared these clinical features in AA, GA, and GG, excluding 6 patients with unilateral MMD, but the results were not changed (data not shown). Among childhood-onset cases (age at onset <15 years), the associations between the c.14576G>A genotype and these clinical features were generally similar, except for bilateral vasculopathy (all genotypes in childhood-onset cases showed bilateral involvement) (figure 3B).

Correlation between variants other than c.14576G>A and clinical phenotype. We also compared the clinical features of patients with MMD with the other variants, except the c.14576G>A variant, with those without (table e-3). Interestingly, none of the c.14576G>A homozygotes had any other variants. The other patients were categorized into 4 groups, who showed at least one of any individual variants without c.14576G>A (as group GG1), no other variant without c.14576G>A (as group GG0), at least one of any other variants with heterozygous c.14576G>A (as group GA1), and no other variant with heterozygous c.14576G>A (as group GA0). Although there were no differences in age at onset between GG1 and GG0 patients, it was lower in GA0 patients than GA1 patients ($p = 0.03$). Median age at onset was 7 years for GA0 and 12 years for GA1. The frequency of infarctions was lower and that of intracerebral hemorrhage was higher in GA1 than in GA0 ($p = 0.02$, OR 0.19, 95% CI 0.04–0.90 and $p = 0.009$, OR 8.3, 95% CI 2.00–34.19). However, when patients with MMD with another variant, which was predicted to be pathogenic by PolyPhen-2[18] or SIFT[19] algorithms, were compared with those without, consistently no differences in any of these clinical features were observed (data not shown). Further analyses with larger numbers of patients are needed to validate this effect.

Anticipation of MMD. In addition, statistical comparisons of clinical features between 5 parent-offspring pairs having the same *RNF213* genotype (heterozygous c.14576G>A) were performed (table e-5). Age at onset was lower in the second generation than in the first generation ($p = 0.04$). Median age at onset was 5 and 37 years, respectively. This result may support the anticipation of MMD as reported previously.[13] Conversely, age at onset was not different between 6 sibling pairs having the same *RNF213* genotype ($p = 0.67$). Median age at onset was 8 years for the older siblings and 12.5 years for the younger ones. There were no differences in other clinical symptoms among patients from the same pedigree.

DISCUSSION We confirmed a strong association between c.14576G>A in *RNF213* and MMD with the larger number of Japanese patients different from those of the previous studies.[14,15] More importantly, this is the first report showing the significant phenotype-genotype correlation. The OR for the heterozygous c.14576G>A was 236 ($p < 0.001$) and could not be exactly calculated for the homozygote (∞). With the assumption that the effects of both heterozygous and homozygous changes on MMD onset were similar, the homozygous c.14576G>A variant would increase the risk with an OR of 259 (95% CI 100–674, $p < 0.001$). However, the effect of the homozygous variant on MMD onset was expected to be much larger than that of the heterozygote because no homozygote was found in a total of 283 normal controls and 132 unaffected family members in this study and 429 normal controls and 28 unaffected family members in the previous study.[14] We also showed that the risk of being diagnosed with MMD with the homozygous variant was more than 78%. Although this variant does not exactly fit the pure Mendelian inheritance pattern because it is observed to some extent in the normal population, this variant might have a much larger effect on the pathogenesis of MMD than the common variants of complex diseases, considering its extremely high OR. This rare variant could be an example of missing heritability, that is, the majority of heritability of complex traits that are unexplained by common variants with a small effect size.[20,21] Thus, this variant should not be considered as one of common variants contributing to common diseases.

The c.14576G>A variant has not been found among the total number of 55 Caucasian patients in the previous studies on *RNF213*.[14,15] However, 4 other rare variants were identified in 4 of 50 Caucasian patients.[15] The overall variant detection rate for *RNF213* was as high as 90.2% for our Japanese patients, in contrast to 8% for the Caucasian patients in the previous study.[15] Importantly, 82.4% of our patients were accounted for by the c.14576G>A variant. It was reported that c.14576G>A variant was identified in 90% of Japanese patients, 79% of Korean patients, and 23% of Chinese patients.[15] The founder effect widely distributed in some areas of east Asia was likely to be expected, and this variant could explain the difference of prevalence of MMD between Asian and non-Asian populations.

RNF213 is a RING (really interesting new gene) finger protein containing an AAA (ATPases associated with variety of a cellular activities) domain, indicating that it has E3 ubiquitin ligase activity and energy-dependent unfoldase activity.[14,22] Knockdown of *RNF213* in zebrafish leads to the abnormal sprouting and irregular diameter of intracranial vessels, suggesting its possible contribution to vascular formation.[15] More research on its contribution to MMD pathogenesis will be necessary.

Although the number of adult-onset cases was relatively small, the similar rates of the cases with this variant between childhood-onset patients and sporadic adult-onset patients might suggest that the variant apparently contributes to both groups. Either a heterozygous or homozygous c.14576G>A variant increased the risk for adult-onset MMD (OR 217,

95% CI 72–656, $p < 0.001$) compared with that in adult normal controls.

Whether bilateral and unilateral MMD belong to a single entity is a very important question. Of the 6 patients with unilateral MMD, 2 were heterozygotes and the others were wild types, which indicated a lower frequency of heterozygotes than that in the previous study.[14] Because we showed a significant difference in the frequency of bilateral vasculopathy between GG and other genotypes, we speculate that to some extent patients with unilateral MMD share a genetic background, but there could be different genetic backgrounds in these groups. Further investigation is needed to confirm these findings with larger numbers of patients with unilateral MMD.

The recent spread of brain check-up has increased the opportunity to encounter patients with asymptomatic MMD.[23] Whereas our patients in this study all had symptomatic MMD, it is necessary to further examine the *RNF213* variant in the asymptomatic group.

The homozygous c.14576G>A variant carriers showed significantly earlier age at onset, more frequent occurrence of infarctions at initial presentation, and PCA involvement. The association of PCA involvement and infarction or intellectual impairment in our data were compatible with the previous report.[11] These features indicate that c.14576G>A homozygotes have more severe and wider vasculopathy in the brain. The other poor prognostic factors, such as intellectual impairment and epilepsy,[8] were probably more frequent in homozygotes but did not reach statistical significance. We speculated that these conditions might be modified or prevented by early diagnosis and by surgical and medical interventions.

Early surgery for young patients with MMD (<3–4 years of age) has been recommended previously,[24] because they often demonstrate a more severe clinical course.[9,10,24] Approximately 80% of these patients had infarction at initial presentation and had subsequent preoperative infarctions more frequently than patients with older age at onset.[24,25] In our study, 77.1% of the patients diagnosed before age 4 had infarctions at diagnosis, whereas 38% of those diagnosed after age 4 had infarctions ($p < 0.001$), results similar to the previous data.

Conversely, it was demonstrated that young age at onset of symptoms did not always herald a poor later outcome. Instead, neurologic deficits due to infarctions at the time of surgery held the most prognostic value.[7,26] It was recently reported that an irreversible infarction was the greatest risk for an unfavorable outcome by multivariate logistic regression analysis.[8] Specific biomarkers, which might be strongly associated with infarction, would be of invaluable clinical importance to provide the appropriate timing for an operation. In our study, 60% of homozygous c.14576G>A individuals were diagnosed with MMD before age 4, and all of them had infarctions at initial presentation. Thus, the homozygous c.14576G>A variant may be a more specific predictor, which would discriminate those with poor prognosis from those with relatively favorable prognosis among patients with young-onset MMD.

We therefore propose that the homozygous c.14576G>A genotype could be an efficient DNA marker predicting the severe type of MMD with a poor prognosis and a strong biomarker for patients requiring early operation. c.14576G>A genotyping could also be useful to predict the actual risk of severe initial infarctions. Careful follow-up of these high-risk homozygotes could make it possible to undertake intervention before the first infarctions and prevent the irreversible neurologic deficits that can occur in these patients. Thus, the homozygous c.14576G>A variants may provide a better monitoring and prevention strategy. Furthermore, this variant could be very useful in genetic counseling.

AUTHOR CONTRIBUTIONS

Dr. Miyatake: study concept and design, analysis of the genetic data, data integrity, interpretation of the data, statistical analysis, and drafting/revising the manuscript. Dr. Miyake: data integrity, interpretation of the data, and drafting/revising the manuscript. Dr. Touho: analysis of the clinical data and sample collection. Dr. Nishimura-Tadaki: analysis of the genetic data. Dr. Kondo: analysis of the genetic data. Dr. Okada: analysis of the genetic data. Dr. Tsurusaki: analysis of the genetic data. Dr. Doi: analysis of the genetic data. Dr. Sakai: analysis of the genetic data. Dr. Saitsu: data integrity, interpretation of the data, and drafting/revising the manuscript. Dr. Shimojima: analysis of the clinical data and sample collection. Dr. Yamamoto: analysis of the clinical data and sample collection. Dr. Higurashi: analysis of the clinical data and sample collection. Dr. Kawahara: analysis of the clinical data, sample collection, and drafting/revising the manuscript. Dr. Kawauchi: analysis of the clinical data and sample collection. Dr. Nagasaka: analysis of the clinical data and sample collection. Dr. Okamoto: analysis of the clinical data and sample collection. Dr. Mori: analysis of the clinical data and sample collection. Dr. Koyano: analysis of the clinical data and sample collection. Dr. Kuroiwa: analysis of the clinical data and sample collection. Dr. Taguri: statistical analysis and drafting/revising the manuscript. Dr. Morita: statistical analysis and drafting/revising the manuscript. Dr. Matsubara: drafting/revising the manuscript. Dr. Kure: drafting/revising the manuscript. Dr. Matsumoto: study concept and design, analysis of the genetic data, data integrity, interpretation of the data, statistical analysis, and drafting/revising the manuscript.

ACKNOWLEDGMENT

The authors thank all the participants for their cooperation in this research; Dr. M. Amamoto, MD, from the Department of Pediatrics, Kitakyushu City Yahata Hospital Critical Care Medical Center, for providing a sample and clinical information for the patient with MMD; and Y. Yamashita, Dr. K. Nishiyama, K. Takabe, T. Miyama, and E. Koike, from the Department of Human Genetics, Yokohama City University Graduate School of Medicine, for their technical assistance.

DISCLOSURE

Dr. Miyatake reports no disclosures. Dr. Miyake is funded by research grants from the Ministry of Health, Labour and Welfare, and a Grant-in-Aid for Young Scientists from the Japan Society for the Promotion of Science. Dr. Touho, Dr. Nishimura-Tadaki, Dr. Kondo, Dr. Okada, Dr. Tsurusaki, Dr. Doi, and Dr. Sakai report no disclosures. Dr. Saitsu is funded by research grants from the Ministry of Health, Labour and Welfare and a Grant-in-Aid for Young Scientists from the Japan Society for the Promotion of Science. Dr. Shimojima reports no disclosures. Dr. Yamamoto is funded by a research grant, Scientific Research (c) from the Japan Ministry of Education, Science, Sports and Culture. Dr. Higurashi, Dr. Kawahara, Dr. Kawauchi, Dr. Nagasaka, Dr. Okamoto, Dr. Mori, Dr. Koyano, Dr. Kuroiwa, Dr. Taguri, Dr. Morita, Dr. Matsubara, and Dr. Kure report no disclosures. Dr. Matsumoto serves on editorial advisory boards for *Clinical Genetics, Journal of Human Genetics*, and *American Journal of Medical Genetics Part A* and is funded by research grants from the Ministry of Health, Labour and Welfare, the Japan Science and Technology Agency, a Grant-in-Aid for Scientific Research on Innovative Areas-(Foundation of Synapse and Neurocircuit Pathology)-from the Ministry of Education, Culture, Sports, Science and Technology of Japan, a Grant-in-Aid for Scientific Research from the Japan Society for the Promotion of Science, and a grant from the Takeda Science Foundation.

Received August 6, 2011. Accepted in final form October 26, 2011.

REFERENCES

1. Bigi S, Fischer U, Wehrli E, et al. Acute ischemic stroke in children versus young adults. Ann Neurol 2011;70:245–254.
2. Mackay MT, Wiznitzer M, Benedict SL, Lee KJ, Deveber GA, Ganesan V. Arterial ischemic stroke risk factors: the International Pediatric Stroke Study. Ann Neurol 2011; 69:130–140.
3. Wakai K, Tamakoshi A, Ikezaki K, et al. Epidemiological features of moyamoya disease in Japan: findings from a nationwide survey. Clin Neurol Neurosurg 1997;99(suppl 2):S1–S5.
4. Kuriyama S, Kusaka Y, Fujimura M, et al. Prevalence and clinicoepidemiological features of moyamoya disease in Japan: findings from a nationwide epidemiological survey. Stroke 2008;39:42–47.
5. Yonekawa Y, Ogata N, Kaku Y, Taub E, Imhof HG. Moyamoya disease in Europe, past and present status. Clin Neurol Neurosurg 1997;99(suppl 2):S58–S60.
6. Kuroda S, Houkin K. Moyamoya disease: current concepts and future perspectives. Lancet Neurol 2008;7:1056–1066.
7. Scott RM, Smith ER. Moyamoya disease and moyamoya syndrome. N Engl J Med 2009;360:1226–1237.
8. Kim SK, Cho BK, Phi JH, et al. Pediatric moyamoya disease: an analysis of 410 consecutive cases. Ann Neurol 2010;68:92–101.
9. Karasawa J, Touho H, Ohnishi H, Miyamoto S, Kikuchi H. Long-term follow-up study after extracranial-intracranial bypass surgery for anterior circulation ischemia in childhood moyamoya disease. J Neurosurg 1992; 77:84–89.
10. Kurokawa T, Tomita S, Ueda K, et al. Prognosis of occlusive disease of the circle of Willis (moyamoya disease) in children. Pediatr Neurol 1985;1:274–277.
11. Yamada I, Himeno Y, Suzuki S, Matsushima Y. Posterior circulation in moyamoya disease: angiographic study. Radiology 1995;197:239–246.
12. Yamauchi T, Houkin K, Tada M, Abe H. Familial occurrence of moyamoya disease. Clin Neurol Neurosurg 1997; 99(suppl 2):S162–S167.
13. Nanba R, Kuroda S, Tada M, Ishikawa T, Houkin K, Iwasaki Y. Clinical features of familial moyamoya disease. Childs Nerv Syst 2006;22:258–262.
14. Kamada F, Aoki Y, Narisawa A, et al. A genome-wide association study identifies RNF213 as the first moyamoya disease gene. J Hum Genet 2011;56:34–40.
15. Liu W, Morito D, Takashima S, et al. Identification of RNF213 as a susceptibility gene for moyamoya disease and its possible role in vascular development. PLoS One 2011; 6:e22542.
16. Fukui M. Guidelines for the diagnosis and treatment of spontaneous occlusion of the circle of Willis ('moyamoya' disease): Research Committee on Spontaneous Occlusion of the Circle of Willis (Moyamoya Disease) of the Ministry of Health and Welfare. Japan Clin Neurol Neurosurg 1997;99(suppl 2):S238–S240.
17. Garritano S, Gemignani F, Voegele C, et al. Determining the effectiveness of high resolution melting analysis for SNP genotyping and mutation scanning at the TP53 locus. BMC Genet 2009;10:5.
18. Adzhubei IA, Schmidt S, Peshkin L, et al. A method and server for predicting damaging missense mutations. Nat Methods 2010;7:248–249.
19. Ng PC, Henikoff S. SIFT: predicting amino acid changes that affect protein function. Nucleic Acids Res 2003;31: 3812–3814.
20. Eichler EE, Flint J, Gibson G, et al. Missing heritability and strategies for finding the underlying causes of complex disease. Nat Rev Genet 2010;11:446–450.
21. Manolio TA, Collins FS, Cox NJ, et al. Finding the missing heritability of complex diseases. Nature 2009;461: 747–753.
22. Lupas AN, Martin J. AAA proteins. Curr Opin Struct Biol 2002;12:746–753.
23. Ikeda K, Iwasaki Y, Kashihara H, et al. Adult moyamoya disease in the asymptomatic Japanese population. J Clin Neurosci 2006;13:334–338.
24. Kim SK, Seol HJ, Cho BK, Hwang YS, Lee DS, Wang KC. Moyamoya disease among young patients: its aggressive clinical course and the role of active surgical treatment. Neurosurgery 2004;54:840–844.
25. Mugikura S, Higano S, Shirane R, Fujimura M, Shimanuki Y, Takahashi S. Posterior circulation and high prevalence of ischemic stroke among young pediatric patients with Moyamoya disease: evidence of angiography-based differences by age at diagnosis. AJNR Am J Neuroradiol 2011;32:192–198.
26. Scott RM, Smith JL, Robertson RL, Madsen JR, Soriano SG, Rockoff MA. Long-term outcome in children with moyamoya syndrome after cranial revascularization by pial synangiosis. J Neurosurg 2004;100:142–149.

Journal of the Neurological Sciences 315 (2012) 77–81

Contents lists available at SciVerse ScienceDirect

Journal of the Neurological Sciences

journal homepage: www.elsevier.com/locate/jns

Hypoperfusion in caudate nuclei in patients with brain–lung–thyroid syndrome

Mitsugu Uematsu [a,*], Kazuhiro Haginoya [b], Atsuo Kikuchi [a], Tojo Nakayama [a], Yousuke Kakisaka [a], Yurika Numata [a], Tomoko Kobayashi [a], Naomi Hino-Fukuyo [a], Ikuma Fujiwara [a], Shigeo Kure [a]

[a] Department of Pediatrics, Tohoku University School of Medicine, Sendai, Japan
[b] Department of Pediatric Neurology, Takuto Rehabilitation Center for Children, Sendai, Japan

ARTICLE INFO

Article history:
Received 20 August 2011
Received in revised form 11 November 2011
Accepted 15 November 2011
Available online 12 December 2011

Keywords:
Brain–lung–thyroid syndrome
NKX2-1
Array CGH
ECD-SPECT
eZIS

ABSTRACT

Mutations in *NKX2-1* cause neurological, pulmonary, and thyroid hormone impairment. Recently, the disease was named brain–lung–thyroid syndrome. Here, we report three patients with brain–lung–thyroid syndrome. All patients were unable to walk until 24 months of age, and still have a staggering gait, without mental retardation. They have also had choreoathetosis since early infancy. Genetic analysis of *NKX2-1* revealed a novel missense mutation (p.Val205Phe) in two patients who were cousins and their maternal families, and a novel 2.6-Mb deletion including *NKX2-1* on chromosome 14 in the other patient. Congenital hypothyroidism was not detected on neonatal screening in the patient with the missense mutation, and frequent respiratory infections were observed in the patient with the deletion in *NKX2-1*. Oral levodopa did not improve the gait disturbance or involuntary movement. The results of ^{99m}Tc-ECD single-photon emission computed tomography (ECD-SPECT) analyzed using the easy Z-score imaging system showed decreased cerebral blood flow in the bilateral basal ganglia, especially in the caudate nuclei, in all three patients, but no brain magnetic resonance imaging (MRI) abnormalities. These brain nuclear image findings indicate that *NKX2-1* haploinsufficiency causes dysfunction of the basal ganglia, especially the caudate nuclei, resulting in choreoathetosis and gait disturbance in this disease.

1. Introduction

NK2 homeobox 1 (*NKX2-1* or *TITF-1*; MIM #600635), which maps on chromosome 14q13, is a member of the *NK-2* gene family of highly conserved homeodomain-containing transcription factors [1,2]. The gene is expressed in the thyroid, bronchial epithelium, and specific areas of the forebrain during development in the mouse [3–5]. Mice homozygous for the disrupted gene are born dead and lack a thyroid gland, lung parenchyma, and pituitary gland, while heterozygous mice develop normally [4]. An abnormality of the gene in humans was first reported in patients with congenital hypothyroidism [6]. Subsequently, heterozygous point mutations in *NKX2-1* were identified in affected members of a family with benign hereditary chorea [7]. Recently, *NKX2-1* was reported as the gene responsible for brain–lung–thyroid syndrome (MIM #610978), which involves symptoms of neurological impairment, pulmonary disorders, and hypothyroidism [8–13]. Respiratory distress during the neonatal period, recurrent respiratory tract infection, and hypothyroidism are common clinical findings. The neurological impairment is characterized by gait disturbance with delayed first walking and choreoathetosis, in the absence of mental retardation or brain magnetic resonance imaging (MRI) abnormalities [13]. However, some affected individuals have had low-average intelligence, learning problems, psychosis and seizures [14–16].

The pathological mechanism of *NKX2-1* haploinsufficiency has been clarified for the hypothyroidism [17] and pulmonary impairment [18,19], but it is still unclear for the neurological symptoms. Most of the neurological deficits, i.e., the gait disturbance and involuntary movements sometimes accompanied with dystonia, dysarthria, action tremor and saccadic abnormalities [20], reflect dysfunction of the control of movement. Therefore, the basal ganglia were considered to be the most important causal lesion [8,14]. The *NKX2-1* null mouse showed severe morphological changes in the basal ganglia, including absence of the globus pallidus and enlargement of the striatum [4]. *NKX2-1* gene expression has been identified as the origin of the pallidum in the mammalian and avian embryonic archistriatum. These studies indicated that *NKX2*-1 is essential for development of the striatum, especially the pallidum rather than the caudate nuclei [5,21,22].

Brain MRI of patients with brain–lung–thyroid syndrome showed no notable abnormalities, except one case report of reduced size and intensity in the pallidum [8]. Previous brain nuclear imaging studies described various findings regarding the basal ganglia, including reduced blood flow in the striatum and thalamus [23], and hypometabolism in the basal ganglia, more prominent in the caudate nuclei [15].

* Corresponding author at: Department of Pediatrics, Tohoku University School of Medicine, 1-1 Seiryo-machi, Aoba-ku, Sendai 980-8574, Japan. Tel: +81 22 717 7287; fax: +81 22 717 7290.
E-mail address: uematsu@bk9.so-net.ne.jp (M. Uematsu).

0022-510X/$ – see front matter © 2011 Elsevier B.V. All rights reserved.
doi:10.1016/j.jns.2011.11.025

Here, we report three patients with brain–lung–thyroid syndrome in whom the diagnosis was confirmed by genetic examinations. We performed brain nuclear image analysis to investigate the causal lesion for the neurological symptoms.

2. Method

2.1. Clinical findings

We studied three patients (5, 6, and 7 years old; one male and two females) with gait disturbance who visited Tohoku University Hospital between 2008 and 2009 (Table 1).

Patient 1 was the second female child of healthy non-consanguineous parents (Fig. 1). She was born at term without neonatal respiratory problems. Congenital hypothyroidism was noted on neonatal screening and she has been given thyroxin replacement therapy since then. After the age of 1.6 years, she developed recurrent respiratory infections and was admitted to hospital five times in one year. She had normal mental development, but delayed gross motor development. She could sit alone at the age of 12 months and first walked at 38 months. A staggering gait persists. Her trunk and extremes were mildly hypotonic and continuous choreoathetosis was observed during wakefulness and exacerbated by stress.

Patients 2 and 3 were cousins via their maternal families (Fig. 1). Patient 2 was the third female and Patient 3 was an only male child. Both sets of non-consanguineous parents were healthy fathers and affected mothers with mild involuntary movement and a history of delayed first walking. Both patients were born at term without any perinatal complications. Congenital hypothyroidism was diagnosed in the neonatal period by screening in Patient 2, but at the age of 5 years in Patient 3, despite a neonatal screening test. Unlike Patient 1, they had no severe respiratory infections during infancy. Similar to Patient 1, first walking was observed at 30 months in Patient 2 and at 24 months in Patient 3. They also have persistent gait disturbance and choreoathetosis without mental retardation. The neurological examinations in all three patients did not detect any abnormalities, such as muscle weakness, abnormal deep tendon reflexes, or cerebellar manifestations.

Brain MRI in all three patients showed normal brain size, form, and intensity, including the basal ganglia. Oral levodopa (20 mg/kg/day) was given to all three patients, but no obvious improvement in the neurological symptoms was observed.

2.2. Brain nuclear image analysis

All three patients underwent single photon emission computed tomography (SPECT) to evaluate brain function at Tohoku University Hospital using technetium-99 m ethyl cysteinate dimer (ECD, approximately 12 MBq/kg of body weight) as the radiotracer. Twenty minutes after the injection, SPECT images were acquired using a PRISM IRIX (Shimadzu, Kyoto, Japan), with a low-energy, high-resolution, fan-beam collimator. In total, 120 projection datum points in a 128×128 matrix were obtained in 20 min. Using an ODYSSEY computer (Shimadzu), tomograms two pixels thick (5.8 mm) were reconstructed after a high-frequency cutoff with a Butterworth filter.

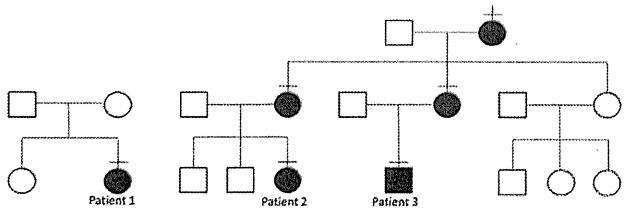

Fig. 1. Family pedigrees of three patients. Affected members are indicated by black squares and circles; unaffected members, white squares and circles. Patient 2 and 3 are cousins on mother's side.

The easy Z-Score Imaging System (eZIS; Fuji Film RI Pharma), used for the statistical analysis of SPECT images, standardizes brain images using Statistical Parametric Mapping (SPM99) [24]. Each SPECT image of the subjects after anatomical standardization followed by isotropic 12-mm smoothing was compared with the mean and SD of SPECT images of the age-matched healthy controls already incorporated in the eZIS program as a normal database using voxel-by-voxel Z-score analysis after voxel normalization to global mean values: Z score = (control mean − individual value)/control SD. These Z-score maps were overlain on tomographic sections and projection with an averaged Z-score of 14-mm thickness to surface rendering of the anatomically standardized MRI template.

Positron emission tomography (PET) was performed in Patients 2 and 3, 1 h after administering [^{18}F]-fluorodeoxyglucose (^{18}FDG) (approximately 3 MBq/kg of body weight) using a Biograph Duo, ECAT EXACT HR^{+} (Siemens, Hoffman Estates, IL) or SET-2400 W (Shimadzu) after fasting for at least 4 h. Emission scans were performed for 10 min for the entire brain. Attenuation was corrected. Fourteen 6-mm-thick slices parallel to the orbitomeatal line, encompassing virtually the entire brain, were analyzed visually by two investigators independently. When the interpretation was inconsistent, a third investigator was called to make a decision.

2.3. Gene analysis

Gene analyses were performed with the informed consent of the patients' parents. Genomic DNA was extracted from peripheral blood lymphocytes using a Sepa Gene kit (Sanko Junyaku, Tokyo, Japan). All coding exons and flanking introns in *NKX2-1* were amplified by PCR. All primers were based on the NCBI reference sequence (accession number NG_013365; the primer sequences are available upon request). The PCR products were separated on 3% agarose gels and purified with a QIAquick Gel Extraction kit (QIAGEN, Chatsworth, CA, USA). The PCR products were sequenced directly using a Big Dye Primer Cycle Sequencing kit and ABI 310 Genetic Analyzer (PE Applied Biosystems, Foster City, CA, USA).

Subsequent array-based comparative genomic hybridization (CGH) analysis was performed using an Agilent 244 K oligonucleotide array (Agilent, Santa Clara, CA; www.agilent.com) with a resolution of approximately 15 kb following the protocols provided by Agilent. The array was analyzed with the Agilent scanner and the Feature Extraction software (v. 9.1.3).

Table 1
Clinical characteristics in three patients.

	Patient 1	Patient 2	Patient 3
Age/sex	7 years/female	5 years/female	6 years/male
Recurrence of respiratory infection	Yes	No	No
Neonatal respiratory problems	No	No	No
Hypothyroidism	Yes (neonatal screening)	Yes (neonatal screening)	Yes (diagnosed at 5 years)
Initiation of walking	3 years and 2 months	2 years and 6 months	2 years
Mental retardation	No	No	No
Choreoathetosis	Yes	Yes	Yes
Response to L-dopa	No	No	No
Brain MRI	Normal	Normal	Normal
NKX2-1 analysis	del 14q12–13	p.V205P	p.V205P

3. Results

From the raw nuclear image ECD-SPECT findings in all three patients (Fig. 2, lower figures) and FDG-PET in Patients 2 and 3